WRDC-TR-89-2112

AUTOMATED CODE DEMONSTRATION FOR COMPRESSOR BLADE STRESSES AND NATURAL FREQUENCIES

Laila Abdel-Dayem
Mark Redding

Stress Technology, Inc.
1800 Brighton-Henrietta Town Line Road
Rochester NY 14623

May 1989

Final Report for Period November 1988 to April 1989

Approved for public release; distribution is unlimited.

AERO PROPULSION AND POWER LABORATORY
WRIGHT RESEARCH AND DEVELOPMENT CENTER
AERONAUTICAL SYSTEMS DIVISION
WRIGHT-PATTERSON AIR FORCE BASE, OHIO 45433-6563

NOTICE

WHEN GOVERNMENT DRAWINGS, SPECIFICATIONS, OR OTHER DATA ARE USED FOR ANY PURPOSE OTHER THAN IN CONNECTION WITH A DEFINITELY GOVERNMENT-RELATED PROCUREMENT, THE UNITED STATES GOVERNMENT INCURS NO RESPONSIBILITY OR ANY OBLIGATION WHATSOEVER. THE FACT THAT THE GOVERNMENT MAY HAVE FORMULATED OR IN ANY WAY SUPPLIED THE SAID DRAWINGS, SPECIFICATIONS, OR OTHER DATA, IS NOT TO BE REGARDED BY IMPLICATION, OR OTHERWISE IN ANY MANNER CONSTRUED, AS LICENSING THE HOLDER, OR ANY OTHER PERSON OR CORPORATION; OR AS CONVEYING ANY RIGHTS OR PERMISSION TO MANUFACTURE, USE OR SELL ANY PATENTED INVENTION THAT MAY IN ANY WAY BE RELATED THERETO.

THIS REPORT HAS BEEN REVIEWED BY THE OFFICE OF PUBLIC AFFAIRS (ASD/PA) AND IS RELEASABLE TO THE NATIONAL TECHNICAL INFORMATION SERVICE (NTIS). AT NTIS IT WILL BE AVAILABLE TO THE GENERAL PUBLIC INCLUDING FOREIGN NATIONS.

THIS TECHNICAL REPORT HAS BEEN REVIEWED AND IS APPROVED FOR PUBLICATION.

Daniel E Thomson

DANIEL E. THOMSON
Project Engineer
Components Branch
Turbine Engine Division

JOHN A. VONADA, Lt Col, USAF
Chief
Components Branch
Turbine Engine Division

FOR THE COMMANDER

Richard J Hill

RICHARD J. HILL
Acting Deputy for Technology
Turbine Engine Division
Aero Propulsion & Power Directorate

IF YOUR ADDRESS HAS CHANGED, IF YOU WISH TO BE REMOVED FROM OUR MAILING LIST, OR IF THE ADDRESSEE IS NO LONGER EMPLOYED BY YOUR ORGANIZATION PLEASE NOTIFY WL/POTC, WRIGHT-PATTERSON AFB, OH 45433-6563 TO HELP MAINTAIN A CURRENT MAILING LIST.

COPIES OF THIS REPORT SHOULD NOT BE RETURNED UNLESS RETURN IS REQUIRED BY SECURITY CONSIDERATIONS, CONTRACTUAL OBLIGATIONS, OR NOTICE ON A SPECIFIC DOCUMENT.

REPORT DOCUMENTATION PAGE

Form Approved
OMB No. 0704-0188

1. AGENCY USE ONLY (Leave blank)	2. REPORT DATE	3. REPORT TYPE AND DATES COVERED
	May 1989	FINAL November 1988 to April 1989

4. TITLE AND SUBTITLE
Automated Code Demonstration for Compressor Blade Stresses and Natural Frequencies

5. FUNDING NUMBERS
F33615-88-C-2900
PR: 3066
TA: 12
WU: 23
PE: 62203F

6. AUTHOR(S)
Laila Abdel-Dayem
Mark Redding

7. PERFORMING ORGANIZATION NAME(S) AND ADDRESS(ES)
Stress Technology Incorporated
1800 Brighton-Henrietta Town Line Road
Rochester NY 14623

8. PERFORMING ORGANIZATION REPORT NUMBER

9. SPONSORING/MONITORING AGENCY NAME(S) AND ADDRESS(ES)
Aero Propulsion and Power Laboratory
Wright Research and Development Center
Aeronautical Systems Division
Wright-Patterson AFB OH 45433-6563

10. SPONSORING/MONITORING AGENCY REPORT NUMBER
WRDC-TR-89-2112

11. SUPPLEMENTARY NOTES
-NONE-

12a. DISTRIBUTION/AVAILABILITY STATEMENT
Approved for public release; distribution is unlimited.

12b. DISTRIBUTION CODE

13. ABSTRACT *(Maximum 200 words)*
Accurate prediction of the stresses, natural frequencies and mode shapes of rotating blades for compressors are essential to the performance of aircraft engines. The first objective of this project is to demonstrate that a preprocessor for the modeling of compressor blades with a wedge type root attachment is feasible. A user-friendly program was devised to be used with the minimum possible input that describes the geometry of different components. This program is called Blade Life Analysis and Design Evaluation (BLADE). The second objective was to run a sample blade through the BLADE software and compare the results with the ANSYS finite element program.

14. SUBJECT TERMS
computer graphics, structural analysis, finite elements

15. NUMBER OF PAGES
52

16. PRICE CODE

17. SECURITY CLASSIFICATION OF REPORT	18. SECURITY CLASSIFICATION OF THIS PAGE	19. SECURITY CLASSIFICATION OF ABSTRACT	20. LIMITATION OF ABSTRACT
UNCLASSIFIED	UNCLASSIFIED	UNCLASSIFIED	UL

ACKNOWLEDGMENT

Stress Technology Incorporated wishes to express its appreciation to the Wright Research and Development Center, Aero Propulsion and Power Laboratory for their financial support that was needed to complete the program as well as the case study analysis. It extends its appreciation to Mr. Ted Fecke and Mr. Dan Thomson for their valuable advice.

TABLE OF CONTENTS

1. INTRODUCTION 1

2. FINITE ELEMENT MODEL 2

   2.1 User Input 2

   2.2 Example 9

3. BLADE ANALYSIS 25

   3.1 Steady Stress Analysis 25

   3.2 Natural Frequency Analysis 30

   3.3 Comparison with Test Results 38

4. CONCLUSION 49

APPENDIX 51

LIST OF FIGURES

		Page
Figure 2.1.1	Typical Airfoil Section Input	4
Figure 2.1.1	Root Side View	6
Figure 2.1.3	Root Front View	7
Figure 2.1.4	Disk Side View	8
Figure 2.2.1	Root Section Front View	11
Figure 2.2.2	Root Section Side View	12
Figure 2.2.3	Disk Data	13
Figure 2.2.4	Example Finite Element Model	17
Figure 2.2.5	Finite Element Model for the Example	18
Figure 2.2.6	Finite Element Model of Root and Disk Section	19
Figure 2.2.7	Finite Element Model for Root	20
Figure 2.2.8	Finite Element Model for Airfoil and Platform	21
Figure 2.2.9	Finite Element Model for Disk Side View	22
Figure 2.2.10	Finite Element Model for Disk Front View	23
Figure 3.1.1	Maximum Nodal Steady Stresses	26
Figure 3.1.2	Maximum Nodal Stresses in Disk	27
Figure 3.1.3	A Different View of Disk Nodal Stresses	28
Figure 3.2.1	Mode Shape 1	32
Figure 3.2.2	Mode Shape 2	33
Figure 3.2.3	Mode Shape 3	34
Figure 3.2.4	Mode Shape 4	35
Figure 3.2.5	Mode Shape 5	36
Figure 3.2.6	Campbell Diagram	37
Figure 3.3.1	Comparison of Test Holograms and Analytical Results for Mode 1	41
Figure 3.3.2	Comparison of Test Holograms and Analytical Results for Mode 2	42
Figure 3.3.3	Comparison of Test Holograms and Analytical Results for Mode 3	43
Figure 3.3.4	Comparison of Test Holograms and Analytical Results for Mode 5	44
Figure 3.3.5	Comparison of Test Holograms and Analytical Results for Mode 6	45

LIST OF FIGURES (CONCLUDED)

Page

Figure 3.3.6 Comparison of Test Holograms and Analytical Results for Mode 8 46

Figure 3.3.7 Comparison of Test Holograms and Analytical Results for Mode 10 47

Figure 3.3.8 Comparison of Test Holograms and Analytical Results for Mode 11 48

LIST OF TABLES

		Page
Table 2.2.1	Example Input File	14
Table 2.2.2	Details of Compressor Blade Model	24
Table 3.1.1	Maximum Equivalent Stresses	29
Table 3.2.1	Natural Frequencies for a Single Blade	31
Table 3.3.1	Comparison of Calculated Frequencies and Test Data	39
Table 3.3.2	Dynamic Modulus of Prototype TI-6AL-4V Blades	40

1. INTRODUCTION

Accurate predictions of the stresses, natural frequencies and mode shapes of rotating blades for compressors are essential to the performance of aircraft engines. The first objective of this project is to demonstrate that a preprocessor for the modeling of compressor blades with a wedge type root attachment is feasible. A user-friendly program was devised to be used with the minimum possible input that describes the geometry of different components.

The second objective was to use this program in conjunction with BLADE to perform steady stress and natural frequency analyses for a selected example. The BLADE program, which is developed by STI, is a special purpose computer code for steam turbine blade stress and fatigue analysis. This program is sponsored by the Electric Power Research Institute (EPRI). A brief description of BLADE is included in the Appendix.

The results of these analyses were evaluated by their comparison to the ANSYS finite element program results. These results were validated using experimental data provided by the Wright Research and Development Center at WPAFB.

2. FINITE ELEMENT MODEL

A finite element model for the blade and disk attachment is constructed with minimum input information on the part of the user. In this section, the user input is described. An example which describes how the finite element model was generated is given.

2.1 User Input

The user should provide the program with some information about the following:

- the vane sections geometry
- the root features
- the disk geometry
- the blade materials
- forcing

The input file is a free format ASCII file. It consists of several records. Each record starts with a keyword which describes the input section for which the next set of data belongs to. The first record of the input file is an exception: it contains the title of the analysis, without being preceded by a keyword. In the following, the input file records are described:

Record 1 : **TITLE**

Record 2 : **COVER** - Keyword
IC - Material reference number
R1 - Radius of blade tip trailing edge
R2 - Radius of blade tip leading edge

Record 3 : **AIRFOIL** - Keyword (Figure 2.1.1)
IA - Material reference number
R - Radius of airfoil section
YLE, ZLE - Coordinates of leading edge
YTE, ZTE - Coordinates of trailing edge

NAP - Number of defined airfoil points on the pressure side

Y(1), Z(1)
.
.
.
Y(2), Z(2). } Pressure side coordinates

Y(NAP), Z(NAP)

NAS - Number of defined airfoil points on the suction side

Y(1), Z(1)
.
.
.
Y(2), Z(2)
Y(NAS), Z(NAS) } Suction side coordinates

Note: NAP and NAS do not have to be equal.
Record 3 may be repeated for different airfoil sections up to a maximum of 10 sections.

Record 4 : PLATFORM - Keyword (Figure 2.1.2)

IP - Material reference number

RØ - Radius to the underside of platform

HD - Height of platform at the downstream end

HU - Height of platform at the upstream end

AL - Axial length of platform

CLE - Distance from root centerline to leading edge of platform

CTE - Distance from root centerline to trailing edge of platform

DC - Distance from platform leading edge to the coordinate axis in the axial direction

OFSET - Offset of root centerline from the blade's global coordinate system

RF - Fillet radius of curvature between the airfoil and platform

ANG - Slant angle

ZERO - The number zero (this variable would be needed for curved roots)

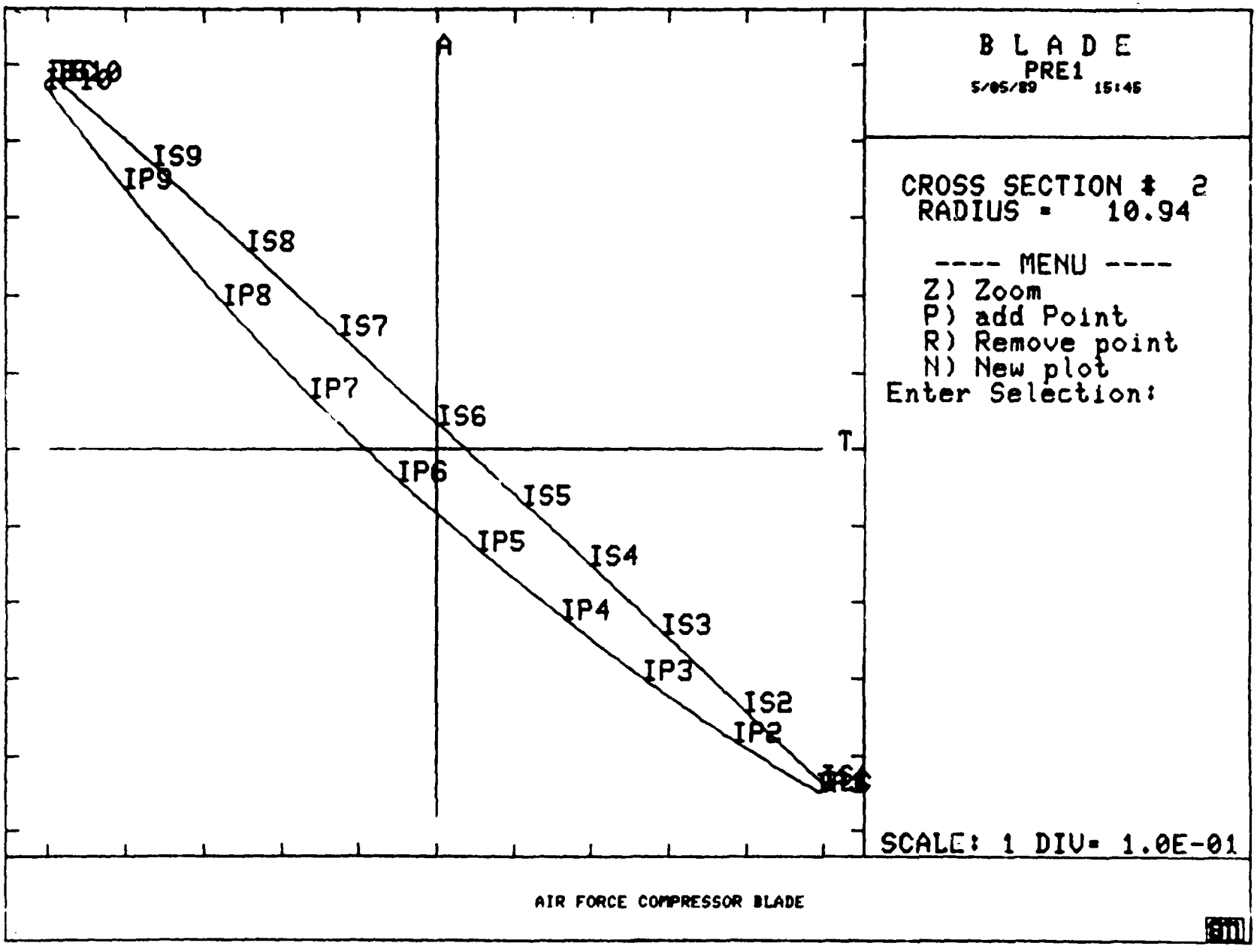

Figure 2.1.1: Typical Airfoil Section Input

Record 5 : **ROOT** - Keyword (Figure 2.1.2 and 2.1.3)

ITYPE - Root type number (set to 61)

IR - Material reference number

X1, Y1,..,
X8,Y8 - Coordinates of input points

R1, R2,
R3, R4 - Input radii

WS - Stop width

NP - Number of points defining root end sections

X(1), Z(1)
X(NP),Z(NP) - Coordinates of end section

Record 6 : **DISC** - Keyword (Figure 2.1.4)

ID - Material reference number

NPD - Number of pair of points describing the disk

X1 (1), Z1 (1), X2 (1), Z2 (1)
X1(NPD),Z1(NPD),X2(NPD),Z2(NPD) - Coordinates of disk points

Record 7 : **MATERIAL** - Keyword

I1 - Material user reference number

IM - Reference number from material library

TM - Temperature at which material is defined

Record 7 may be repeated for different material types up to a maximum of 10 material types.

Record 8 : **STAGE PARAMETERS** - Keyword

NBLADES - Total number of blades in the stage

NBG - Number of blades per group

NGP - Number of groups to be analyzed

NZ - Number of upstream nozzles

DMPR - Damping ratio

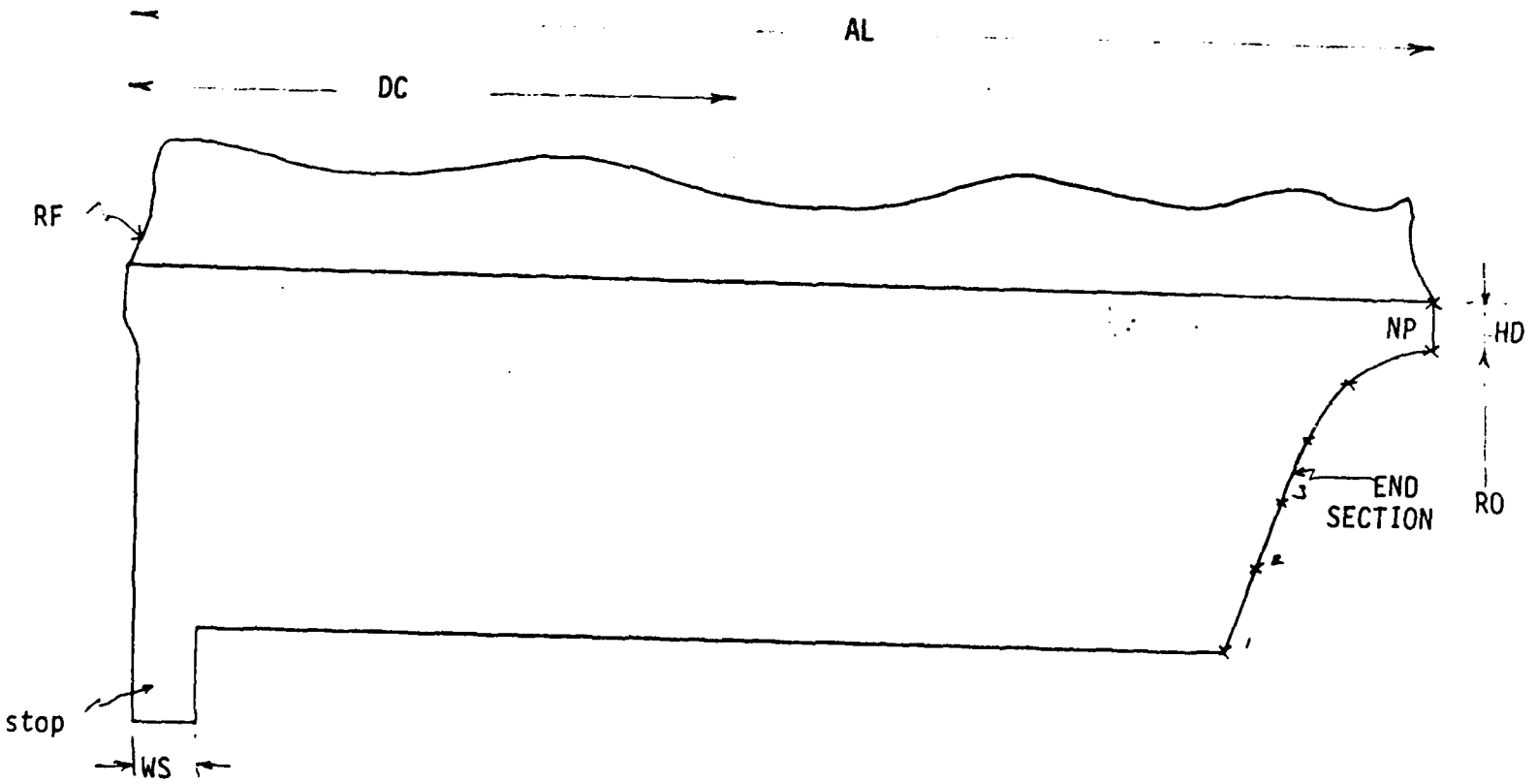

Figure 2.1.2: Root Side View

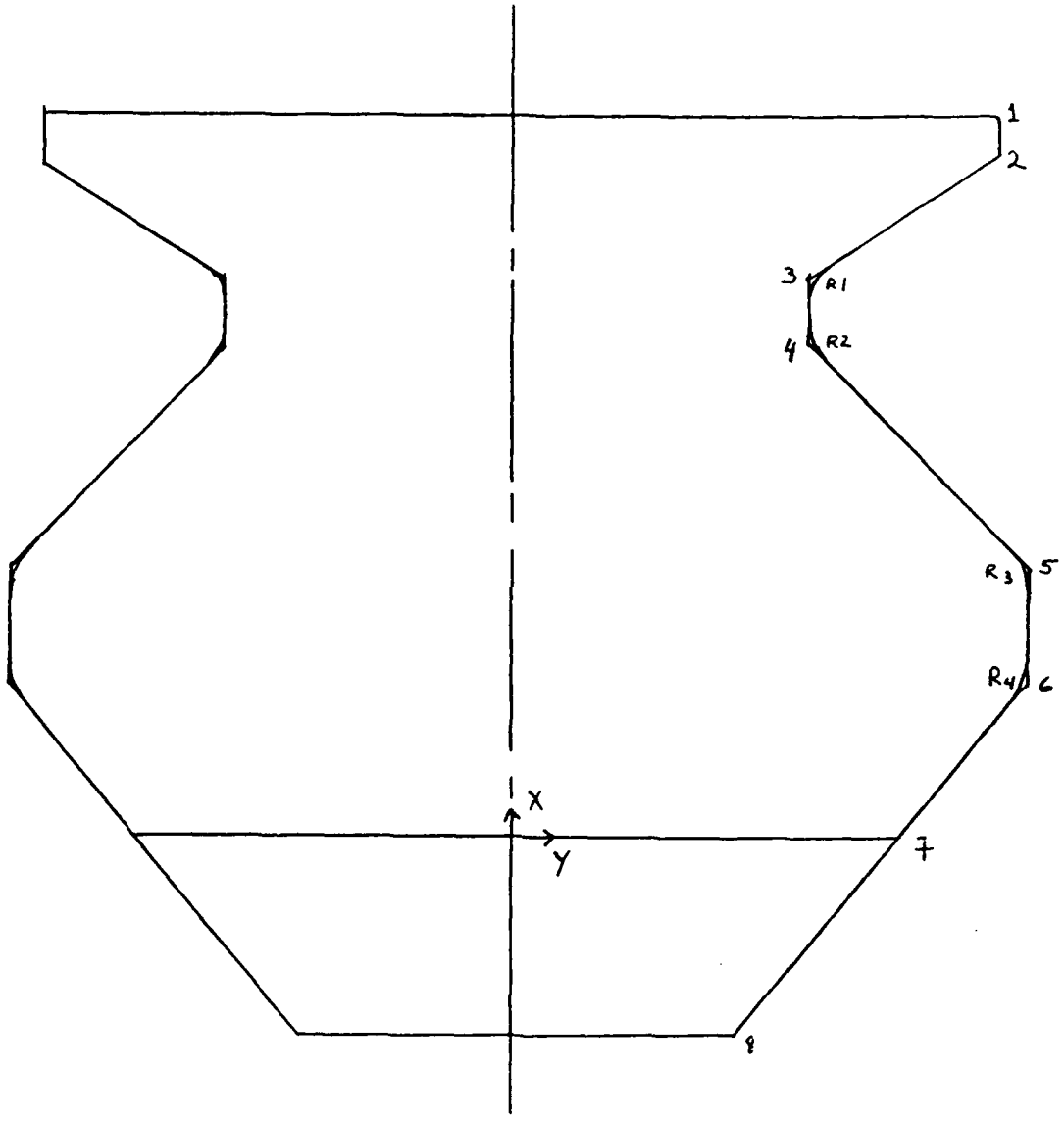

Figure 2.1.3: Root Front View

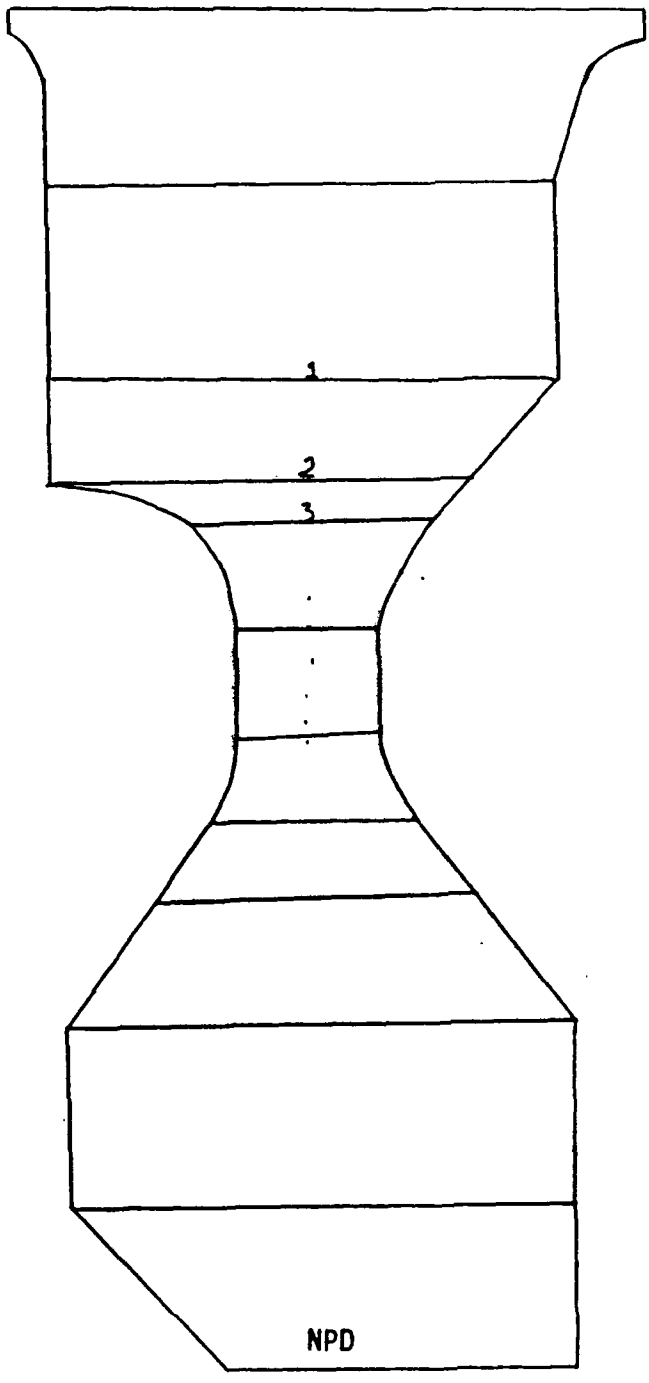

Figure 2.1.4: Disk Side View

	SPEED	-	Rotor speed
	IB	-	Blade of interest for back substitution
Record 9 :	FORCING	-	Keyword
	C	-	
	A1	-	If C = 0.0, tangential stream forces at hub and
	A2		Tip, respectively: otherwise, power of the stage and pressure drop, respectively
	A3	-	If C = 0.0, axial stream forces at hub and tip,
	A4		respectively
Record 10:	EXCITATION	-	Keyword
	NF	-	Number of frequencies to be analyzed for dynamic stresses
	FREQ (1), ST(1), SA(1)	-	First frequency and stimulus ratios in the Tangential and axial direction
	FREQ (NF), ST (nf), SA (nf)	-	Last frequency and stimulus ratios
Record 11:	END	-	Keyword

In the case of natural frequency analysis, records 9 and 10 could be eliminated. They can also be eliminated in the case of steady stress analysis under the effect of centrifugal forces only.

2.2 Example

The blade to be analyzed is the 4th compressor stage of the F100 engine. A typical airfoil profile is given in Figure 2.1.1. Root section information is presented in Figures 2.2.1 and 2.2.2. Figure 2.2.3 shows the disk data and the input file is given in Table 2.2.1.

The finite element model was generated using the preprocessor written by STI for this specific purpose. The finite element meshes for the blade as

well as for the different components are given in Figures 2.2.4 through 2.2.10. Table 2.2.2 gives the number of eight-noded isoparametric finite elements used in modeling each component.

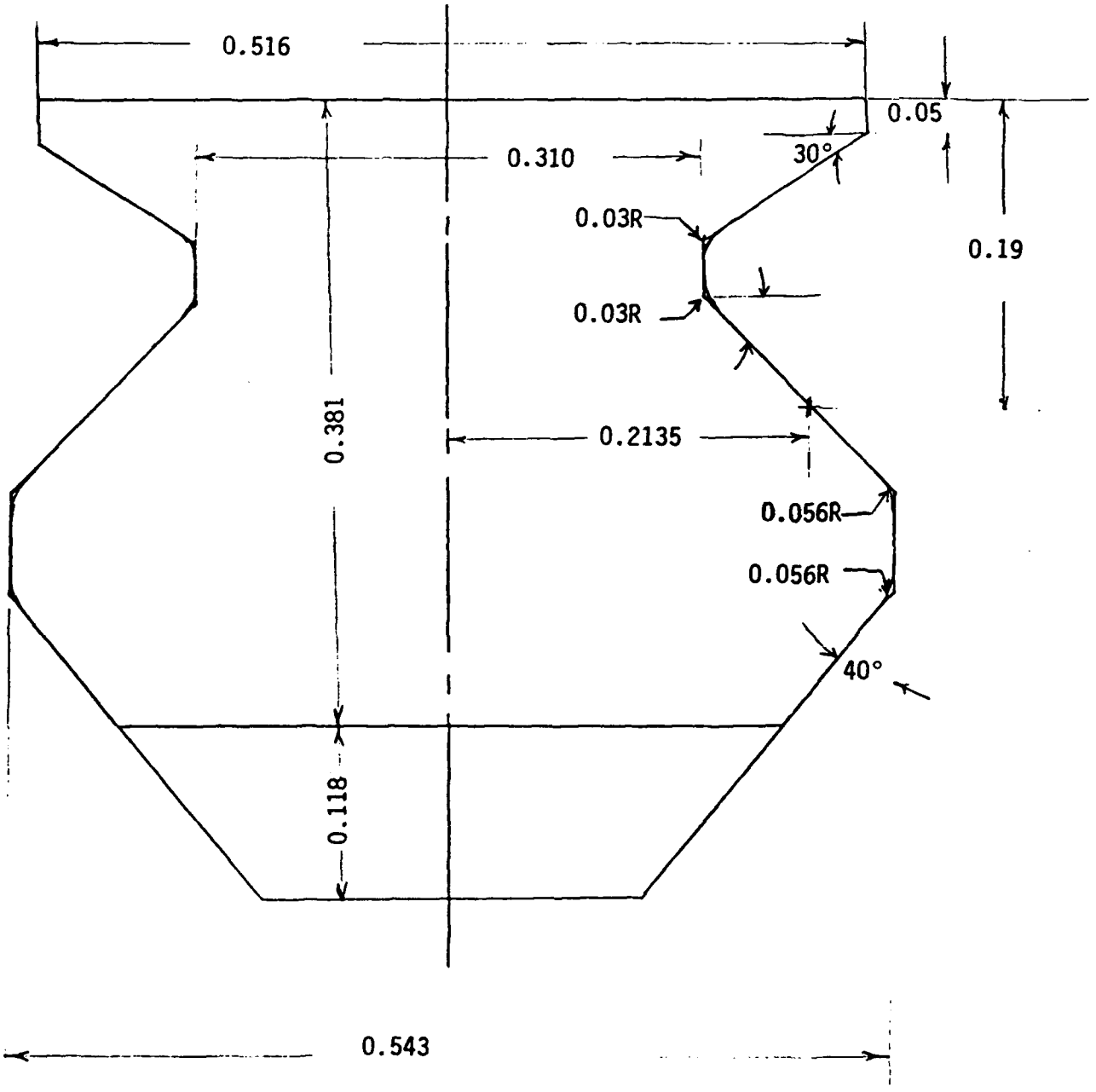

Figure 2.2.1: Root Section Front View

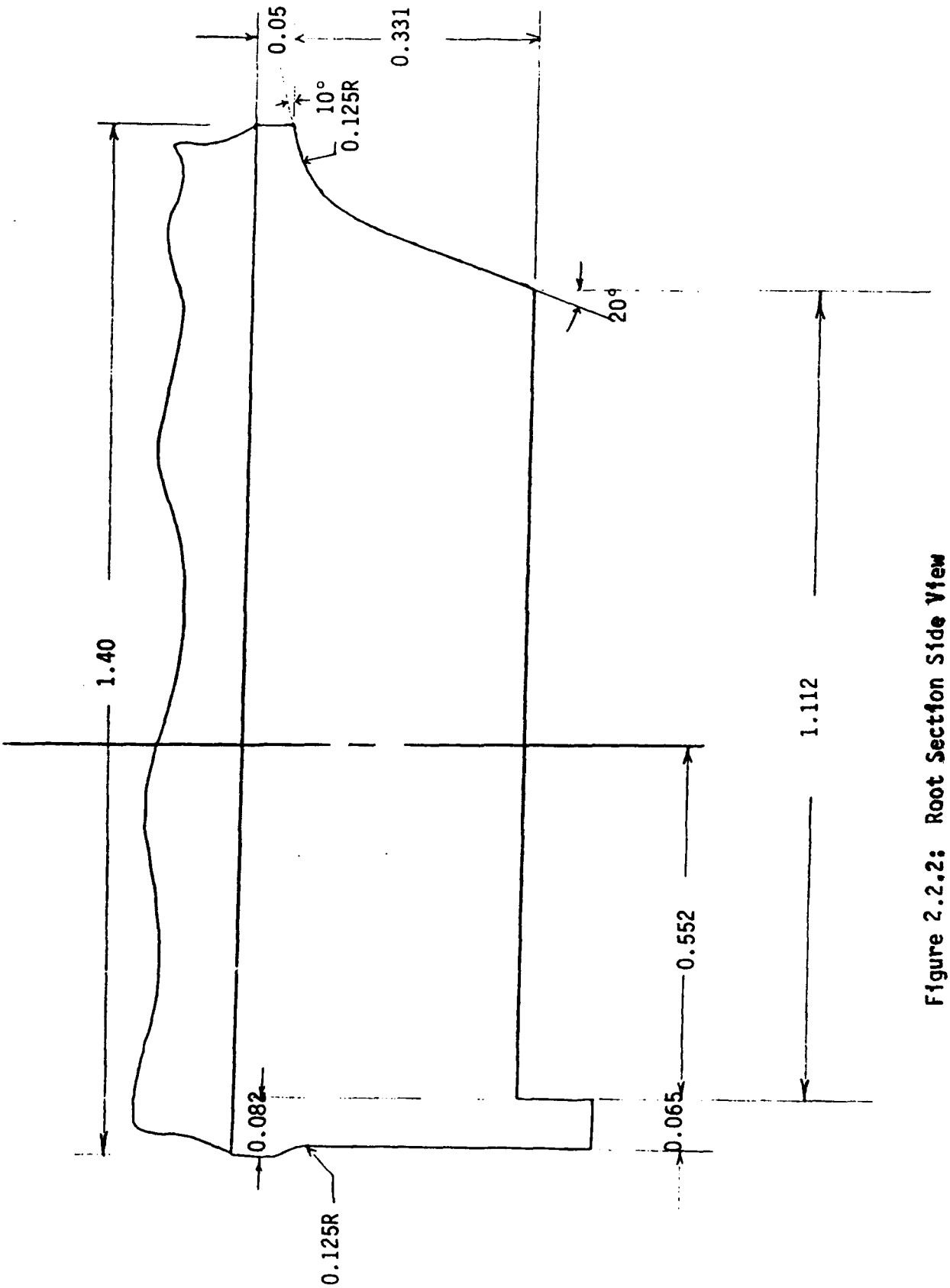

Figure 2.2.2: Root Section Side View

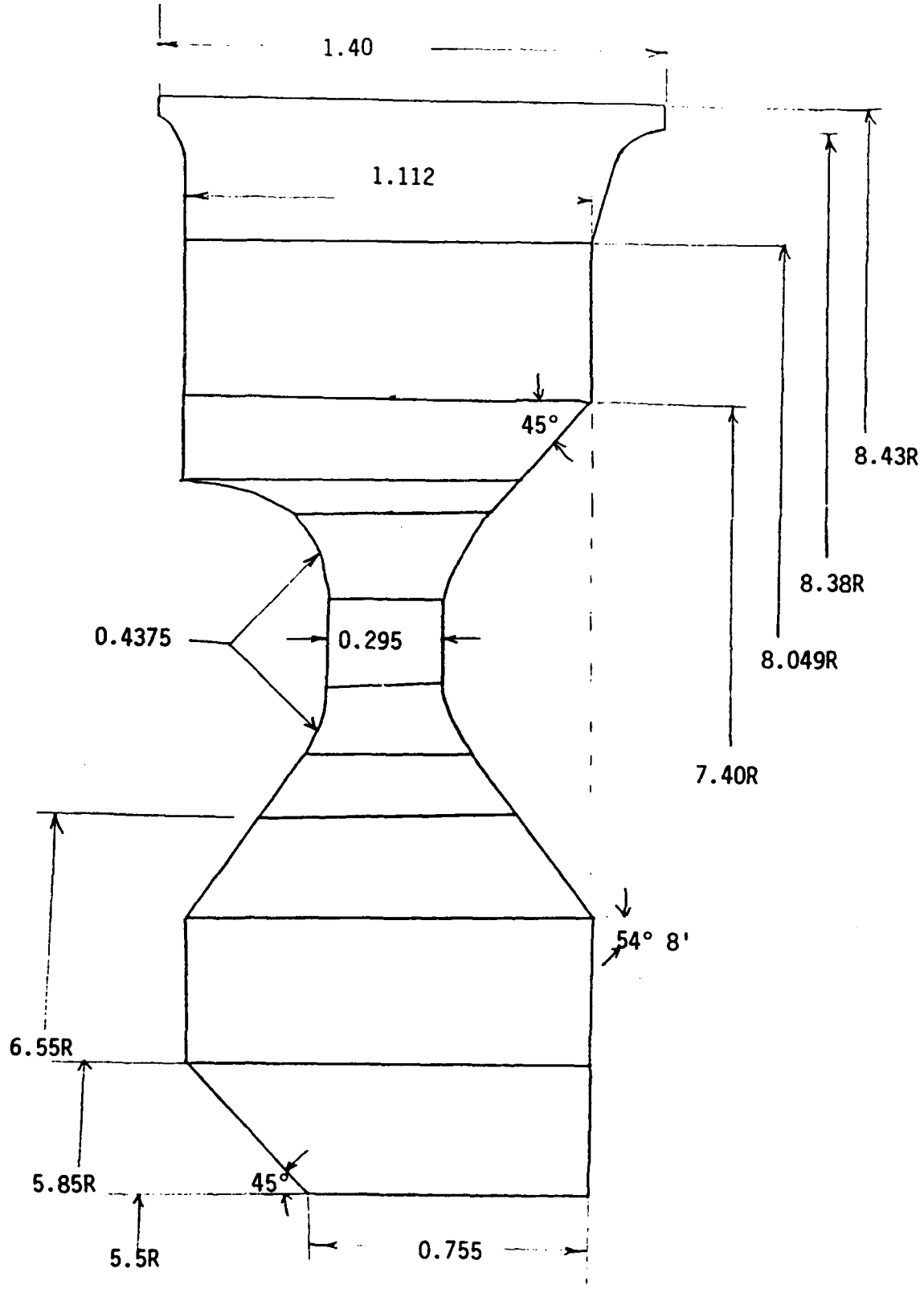

Figure 2.2.3: Disk Data

Table 2.2.1: Example Input File

```
AIR FORCE COMPRESSOR BLADE

COVER
0
11.639   11.729

AIRFOIL
   1
    11.292
    -0.502   -0.394
    +0.510    0.437
    10
    -0.500 -0.386   -0.389 -0.300   -0.286 -0.220   -0.172 -0.130
    -0.072 -0.050   +0.025  0.030   +0.145  0.130   +0.264  0.230
    +0.380  0.330   +0.501  0.437
    10
    -0.495 -0.397   -0.379 -0.330   -0.268 -0.260   -0.150 -0.180
    -0.041 -0.100   +0.070 -0.010   +0.174  0.080   +0.290  0.190
    +0.430  0.330   +0.509  0.430

AIRFOIL
   1
    10.757
    -0.500   -0.445
    +0.502    0.480
    10
    -0.499 -0.437   -0.397 -0.340   -0.292 -0.240   -0.198 -0.150
    -0.112 -0.070    0.000  0.034   +0.125  0.150   +0.245  0.260
    +0.366  0.370   +0.490  0.480
    10
    -0.491 -0.447   -0.383 -0.380   -0.268 -0.300   -0.162 -0.220
    -0.052 -0.130   +0.050 -0.039   +0.163  0.070   +0.276  0.190
    +0.404  0.340   +0.5025 0.469

AIRFOIL
   1
    10.383
    -0.497   -0.479
    +0.487    0.517
    10
    -0.496 -0.469   -0.430 -0.398   -0.300 -0.259   -0.205 -0.160
    -0.118 -0.070   -0.020  0.030   +0.089  0.140   +0.210  0.260
    +0.332  0.380   +0.473  0.516
    10
    -0 486 -0.480   -0.359 -0.400   -0.240 -0.310   -0.141 -0.230
    -0.039 -0.140   +0.064 -0.040   +0.184  0.090   +0.292  0.220
    +0.397  0.360   +0.488  0.500
```

Table 2.2.1: Example Input File (Con't)

```
AIRFOIL
  1
   9.848
  -0.492  -0.524
  +0.451   0.579
  10
  -0.490 -0.512  -0.430 -0.440  -0.330 -0.320  -0.230 -0.200
  -0.130 -0.080  -0.026  0.044  +0.090  0.180  +0.220  0.330
  +0.320  0.445  +0.435  0.577
  10
  -0.480 -0.521  -0.360 -0.449  -0.244 -0.360  -0.140 -0.270
  -0.030 -0.163  +0.080 -0.041  +0.200  0.112  +0.310  0.280
  +0.389  0.420  +0.456  0.563

AIRFOIL
  1
   9.527
  -0.491  -0.546
  +0.423   0.612
  10
  -0.491 -0.533  -0.399 -0.420  -0.301 -0.300  -0.196 -0.170
  -0.091 -0.040  +0.004  0.080  +0.106  0.210  +0.206  0.340
  +0.325  0.500  +0.406  0.609
  10
  -0.480 -0.546  -0.360 -0.470  -0.233 -0.370  -0.120 -0.260
  -0.000 -0.142  +0.107 -0.010  +0.211  0.140  +0.292  0.280
  +0.370  0.440  +0.429  0.596

AIRFOIL
  1
   9.046
  -0.484  -0.568
  +0.365   0.656
  10
  -0.484 -0.554  -0.370 -0.417  -0.291 -0.320  -0.188 -0.190
  -0.093 -0.060  +0.004  0.080  +0.096  0.220  +0.183  0.360
  +0.264  0.500  +0.345  0.650
  10
  -0.471 -0.569  -0.330 -0.480  -0.207 -0.380  -0.095 -0.270
  +0.010 -0.150  +0.117  0.000  +0.208  0.160  +0.279  0.320
  +0.330  0.470  +0.370  0.640
```

Table 2.2.1: Example Input File (Con't)

```
AIRFOIL
  1
    8.725
   -0.474   -0.588
   +0.291    0.695
   10
   -0.473 -0.571   -0.377 -0.460   -0.285 -0.350   -0.190 -0.225
   -0.091 -0.080   -0.000  0.070   +0.081  0.220   +0.162  0.390
   +0.233  0.540   +0.276  0.686
   10
   -0.460 -0.586   -0.335 -0.510   -0.210 -0.420   -0.105 -0.310
   +0.011 -0.170   +0.113 -0.010   +0.194  0.160   +0.257  0.350
   +0.291  0.530   +0.302  0.682

PLATFORM
  1
  8.372  0.050  0.050  1.402  0.2764 0.2764 0.634  0  0.172
  21.0   0

ROOT
    61  1
 0.3925  0.2764   0.3425  0.2764   0.3030  0.1660   0.2625  0.1660
 0.1595  0.2908   0.0806  0.2908   0.0000  0.2287  -0.1065  0.1226
 0.0300  0.0300   0.0560  0.0560
 0.0820
 7
 0.0000  1.1935   0.2105  1.2701   0.2268  1.2760   0.2850  1.3105
 0.3000  1.3252   0.3425  1.4020   0.3925  1.4020

DISC
    1    10
7.5950  0.5595   7.5950 -0.5520   7.4000  0.3574   7.4000 -0.5520
7.3292  0.2796   7.3292 -0.2980   7.1200  0.1515   7.1200 -0.1435
6.9516  0.1515   6.9516 -0.1435   6.6946  0.2351   6.6946 -0.2271
6.5500  0.3534   6.5500 -0.3320   6.2457  0.5530   6.2457 -0.5520
5.8500  0.5530   5.8500 -0.5520   5.5000  0.5530   5.5000 -0.2020

MATERIAL
  1
 3707
  300

STAGE
  52  1  0  60
0.002  6000  1

END
```

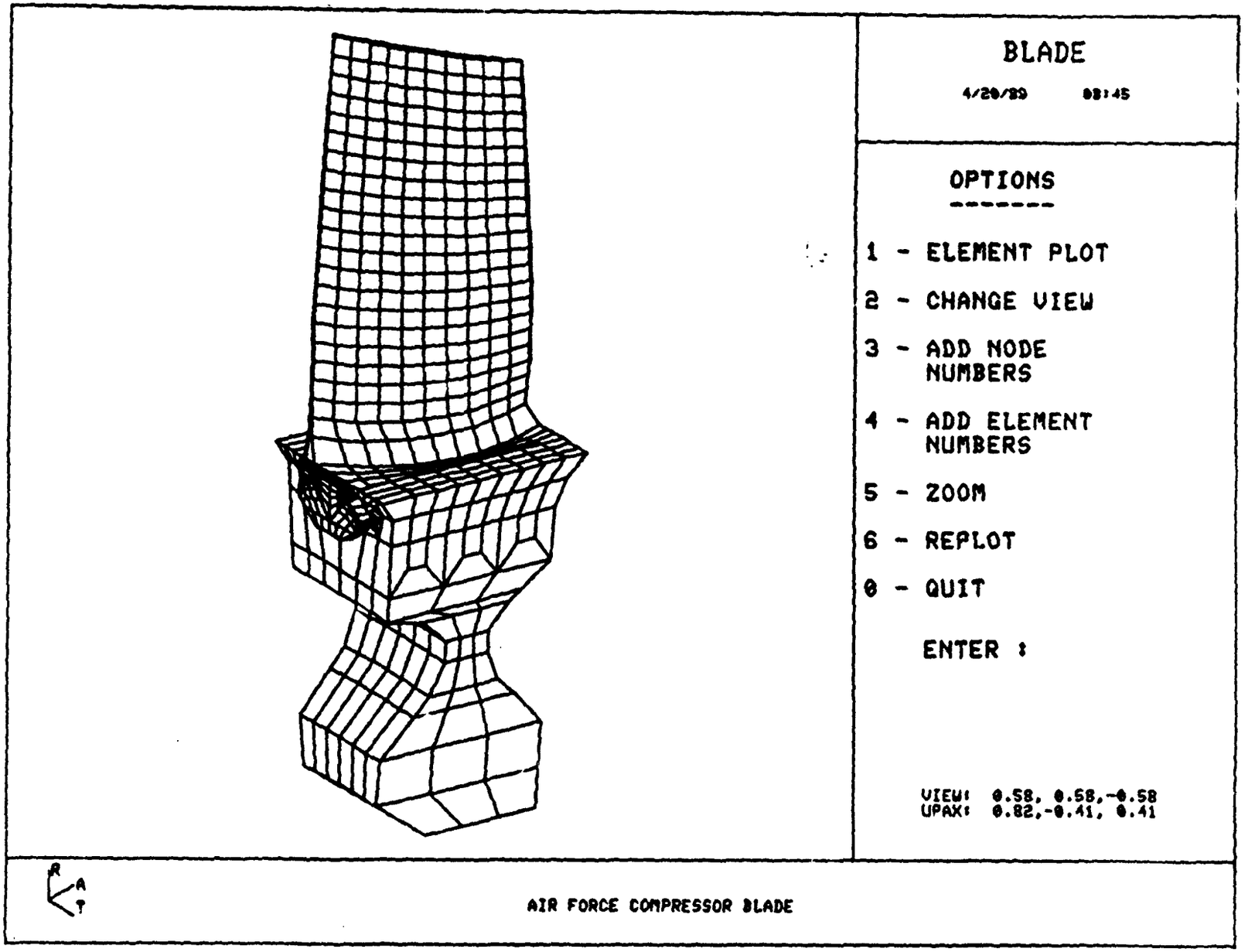

Figure 2.2.4: Example Finite Element Model

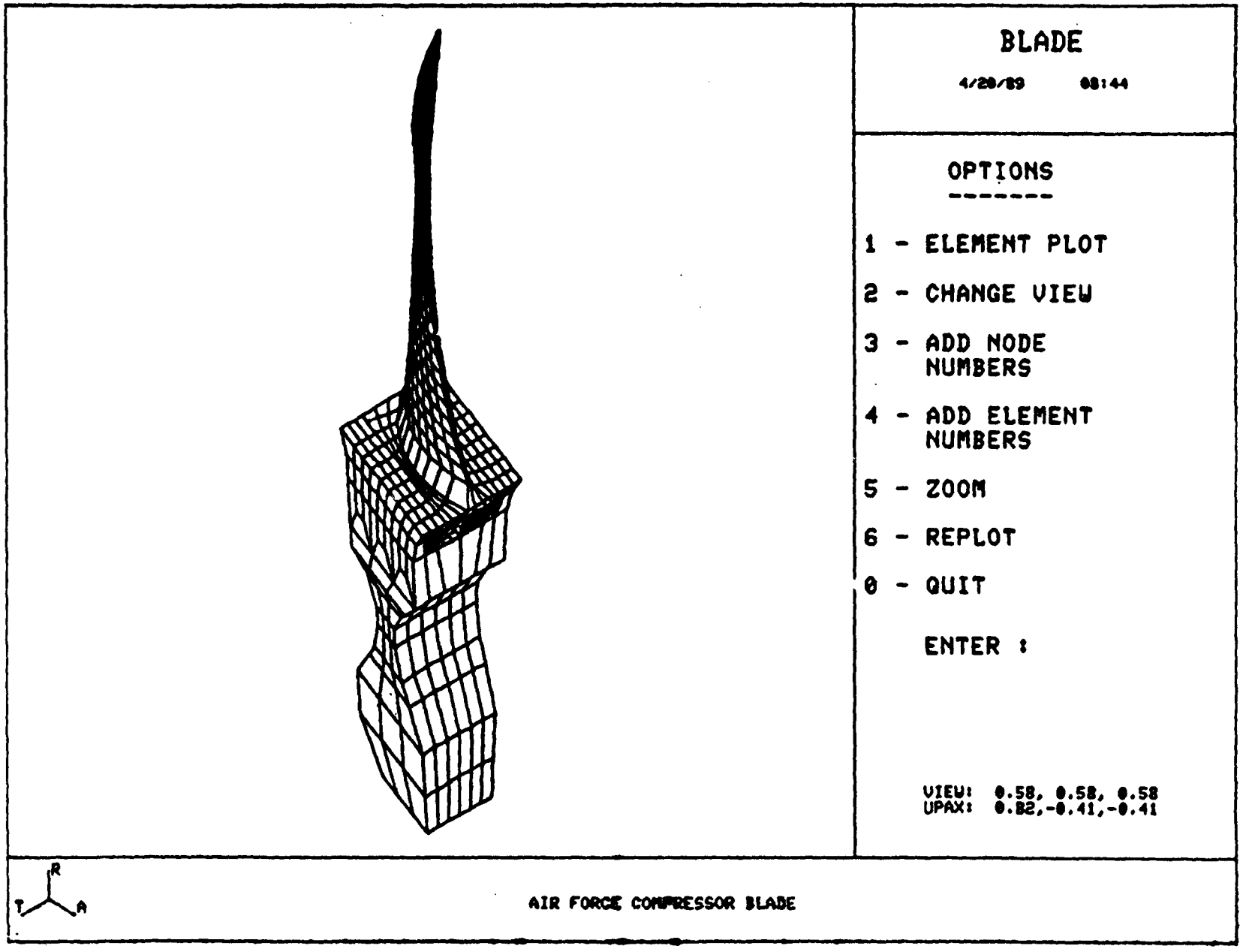

Figure 2.2.5: Finite Element Model for the Example

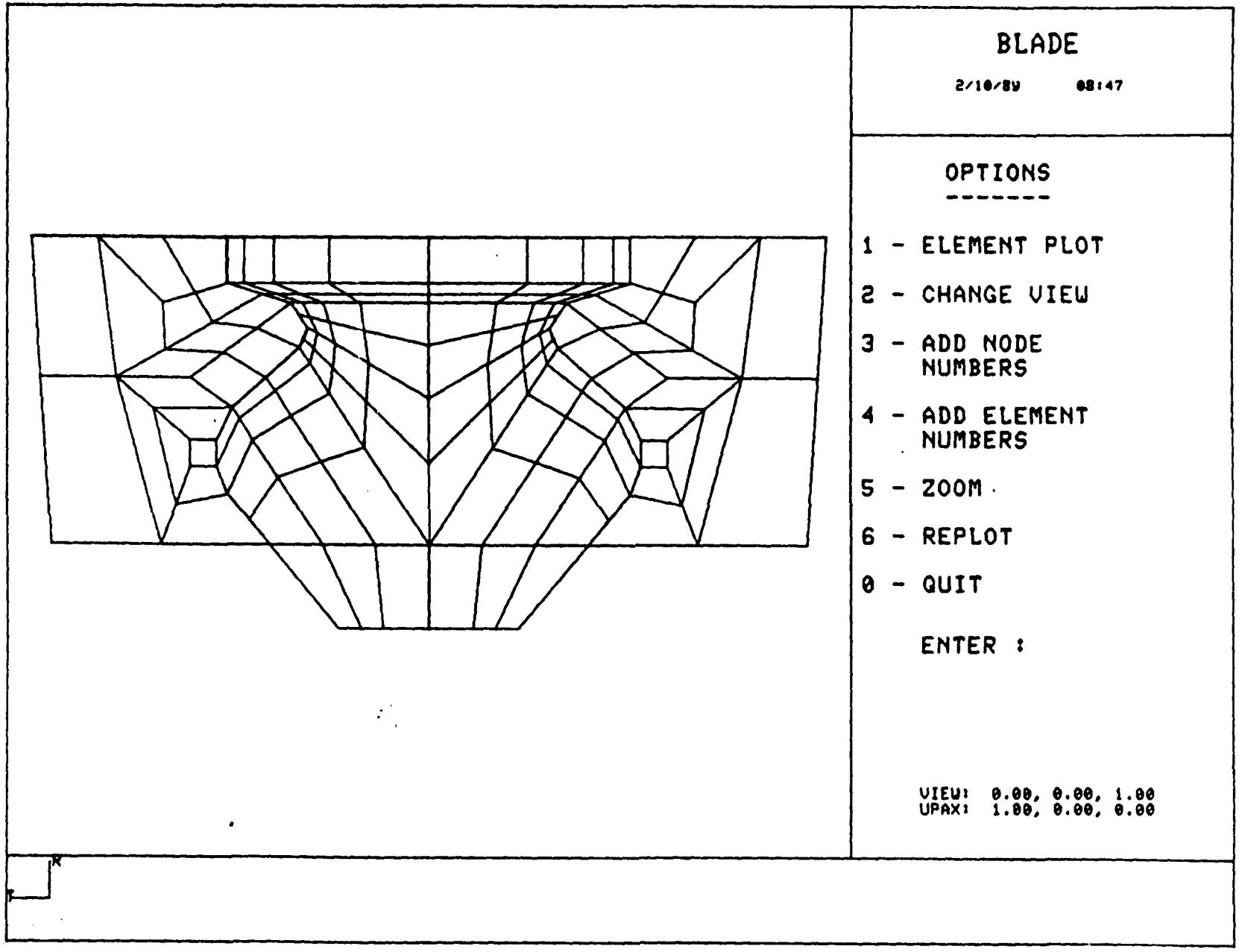

Figure 2.2.6: Finite Element Model of Root and Disk Section

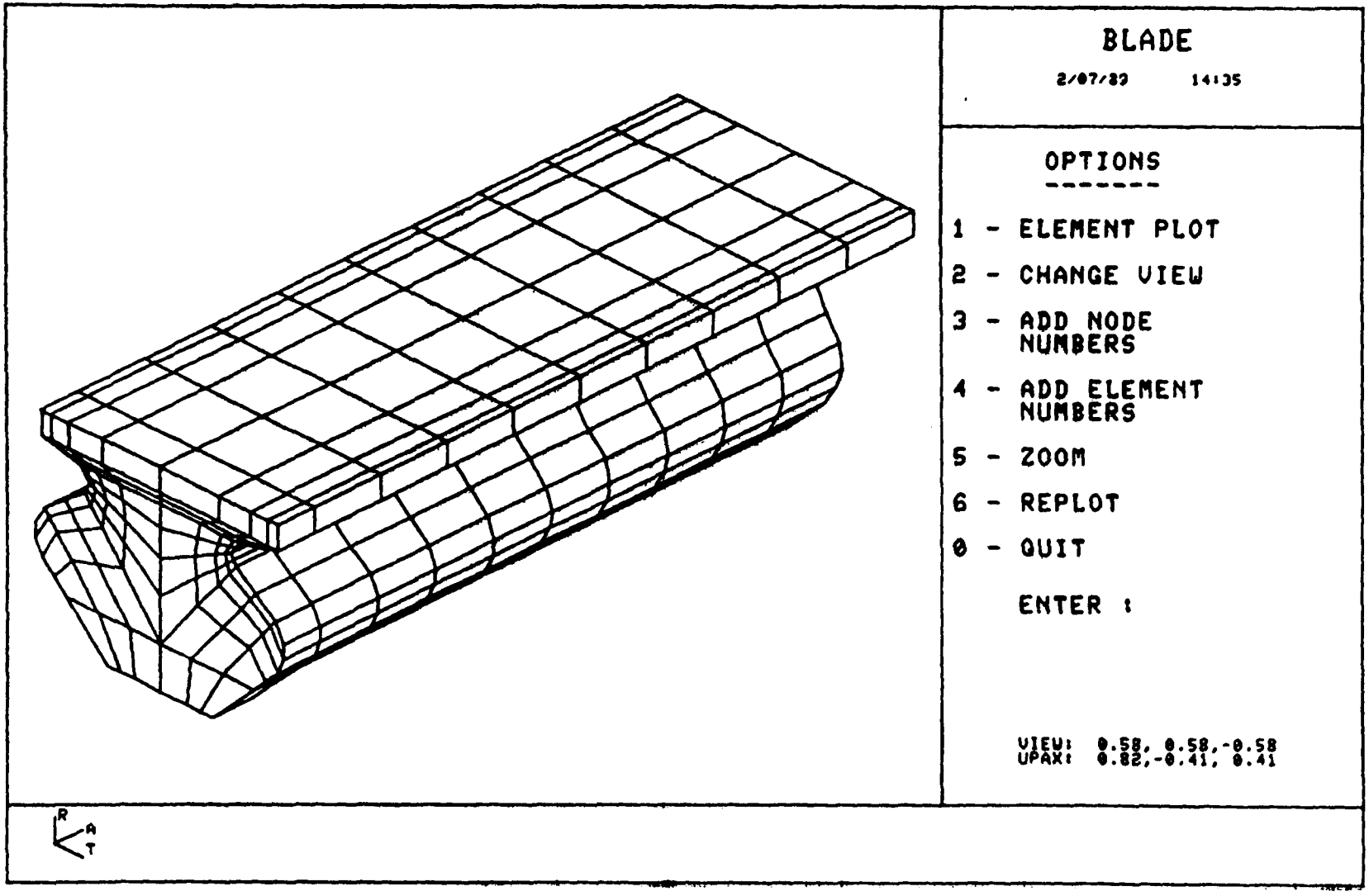

Figure 2.2.7: Finite Element Model for Root

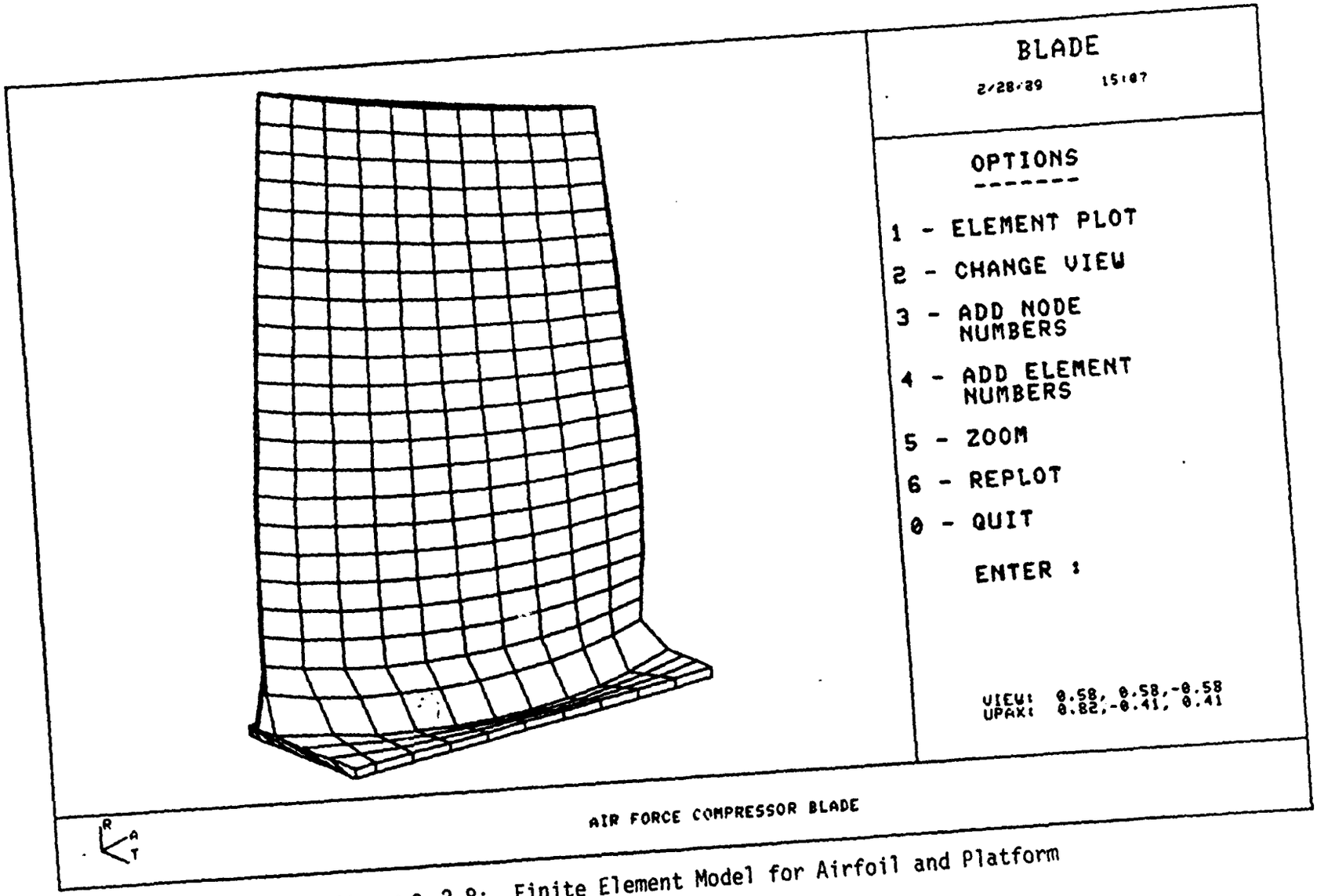

Figure 2.2.8: Finite Element Model for Airfoil and Platform

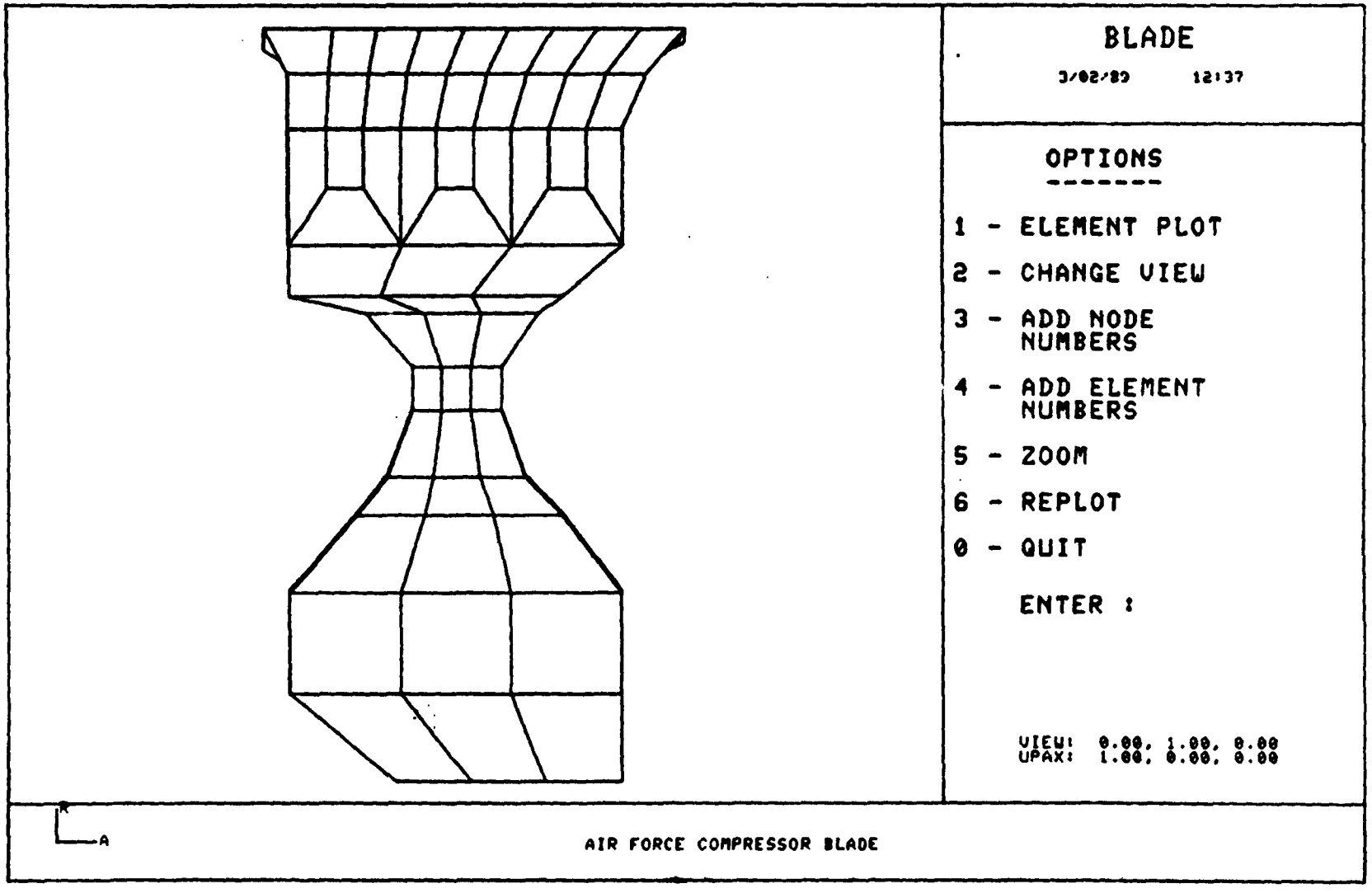

Figure 2.2.9: Finite Element Model for Disk Side View

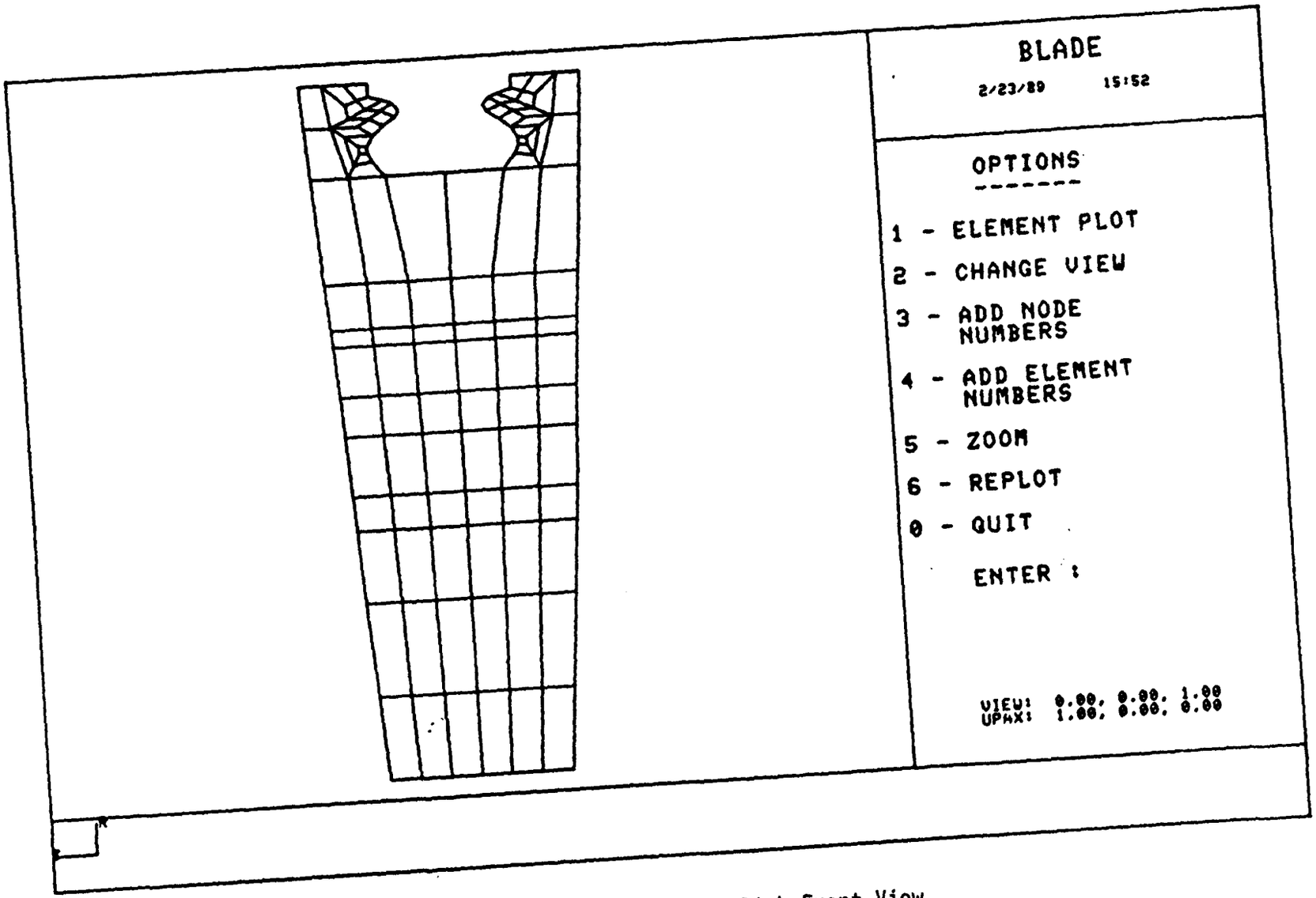

Figure 2.2.10: Finite Element Model for Disk Front View

Table 2.2.2: Details of Compressor Blade Model

Component	Number of elements
Airfoil	440
Platform	80
Root	726
Disk	594
Total	1840

3. BLADE ANALYSIS

The blade underwent two types of analysis, namely steady stress and natural frequencies analyses. Finite element programs ANSYS and BLADE were utilized to perform the computations. Both programs produced identical results which validate the BLADE program.

3.1 Steady Stress Analysis

The blade was analyzed statically under the effect of centrifugal forces. These forces result from the rotation of the rotor. A speed of 6000 rpm was used in the computation. Steady stress variations are shown in Figures 3.1.1 through 3.1.3. Maximum stress values are given in Table 3.1.1.

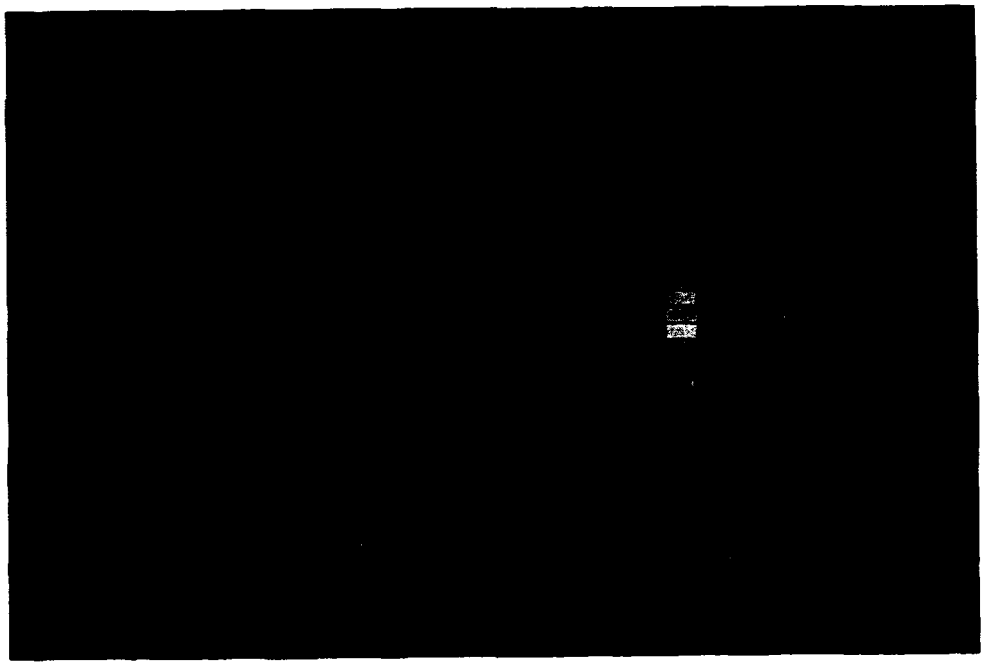

Figure 3.1.1: Maximum Nodal Steady Stresses

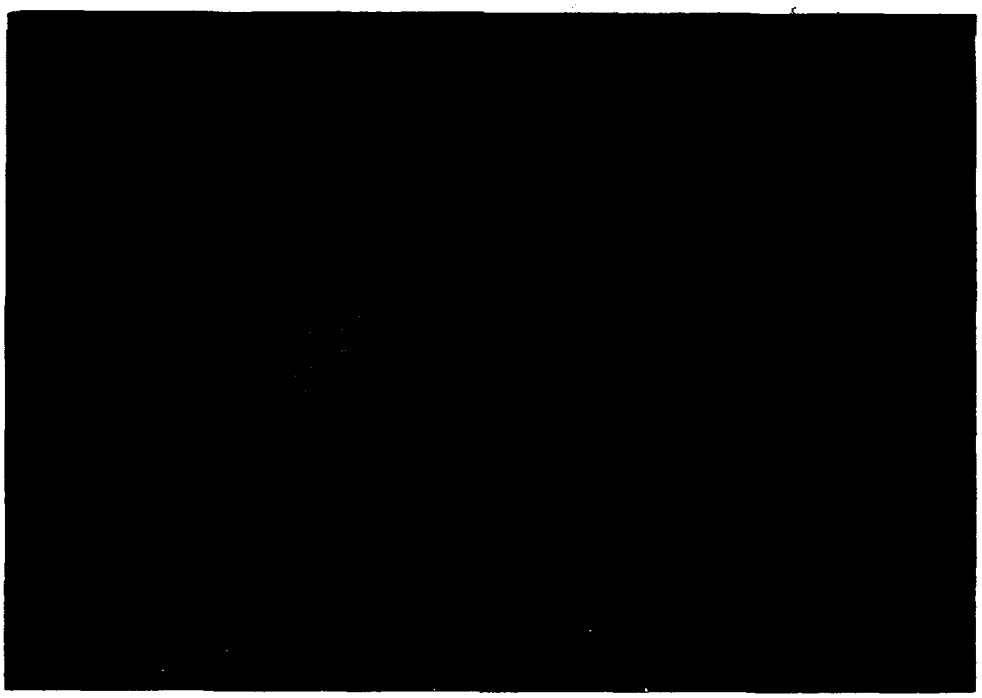

Figure 3.1.2: Maximum Nodal Stresses in Disk

Figure 3.1.3: A Different View of Disk Nodal Stresses

Table 3.1.1 : Maximum Equivalent Stresses

Element #	Location	Stresses, psi	
		BLADE	ANSYS
1358	Disk	10085	10085
1359	Disk	8604.5	8604.5
1546	Disk	8460.0	8460.0
1361	Disk	8411.1	8411.1
1362	Disk	8375.8	8375.8
1360	Disk	8315.4	8315.4

Maximum equivalent stress in:

	BLADE	ANSYS
Airfoil	4364.9 psi	4364.9 psi
Platform	2530.9 psi	2530.9 psi
Root	7569.0 psi	7569.0 psi

3.2 Natural Frequency Analysis

Natural Frequency Analysis was performed on the blade model. The equation of motion for free vibration is of the eigenvalue type,

$$[M]\{\ddot{X}\} + [K]\{X\} = 0$$

where [M] and [K] are the mass and stiffness matrices and {X} is the displacement vector. By solving this eigenvalue problem, the eigenvectors are the mode shapes while the eigenvalues yield the natural frequencies. Due to the large number of degrees of freedom describing the model, Guyan reduction technique was implemented. At operation speed, centrifugal stresses stiffen the blade and therefore the natural frequencies at speed become higher than their corresponding values at zero rpm. The frequency values at speed and at zero rpm are given in Table 3.2.1. Mode shapes are presented in Figures 3.2.1 through 3.2.5. A Campbell diagram which shows the effect of speed on the values of the natural frequencies is given in Figure 3.2.6.

Table 3.2.1 : Natural Frequencies for a Single Blade

Mode #	Frequency (hz)		
	ANSYS	BLADE	
	at 0 rpm	at 0 rpm	at 6000 rpm
1	611.0	611.0	657.6
2	2173.8	2173.8	2212.8
3	2610.6	2610.6	2625.8
4	2854.3	2854.8	2866.6
5	4939.8	4939.8	4969.9
6	5466.2	5466.2	5502.3
7	8565.8	8565.8	8597.4
8	9313.4	9313.4	9347.1
9	10247.0	10247.0	10257.6
10	11118.0	11118.0	11141.9
11	12865.0	12865.0	12902.0

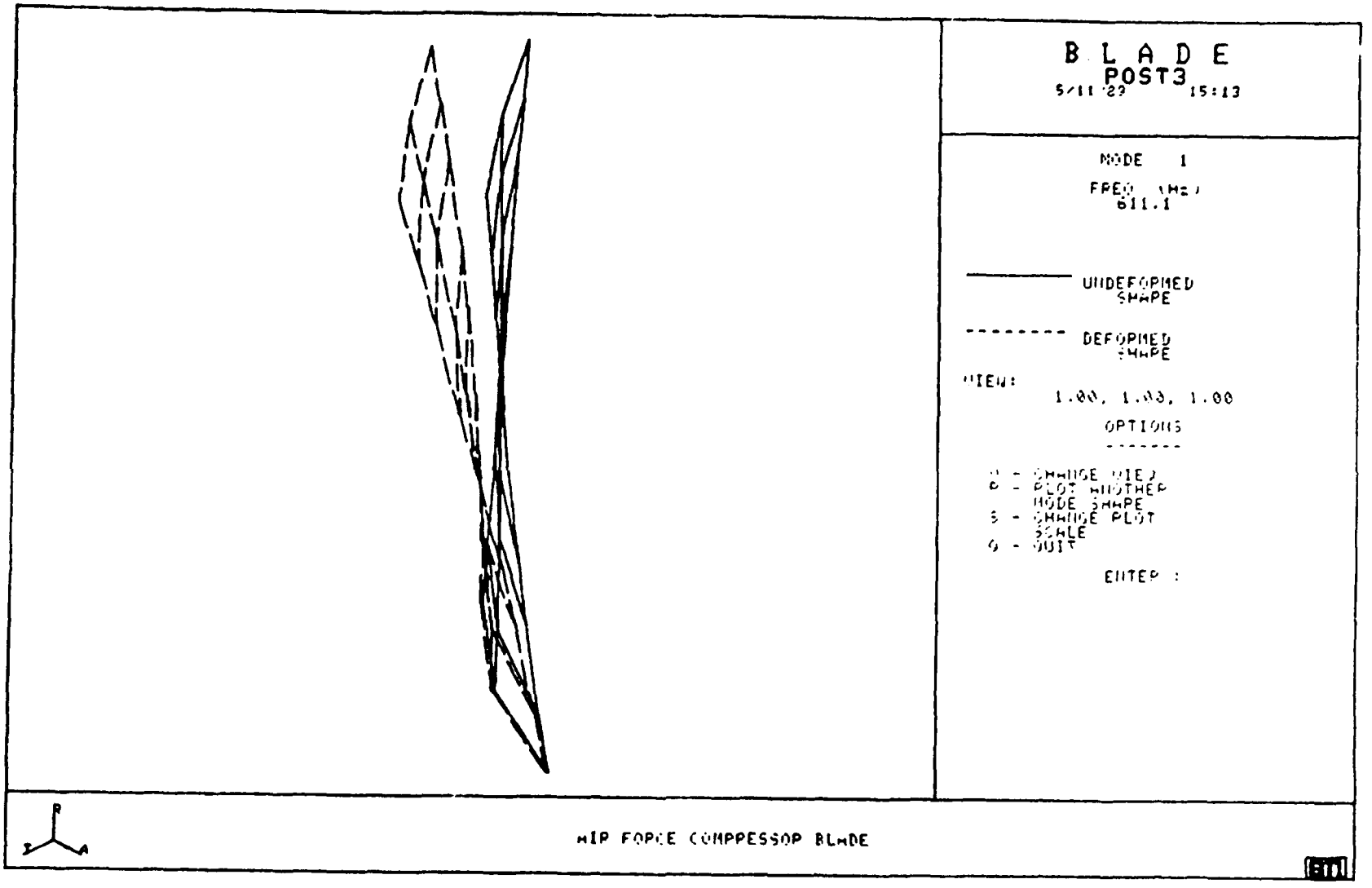

Figure 3.2.1: Mode Shape 1

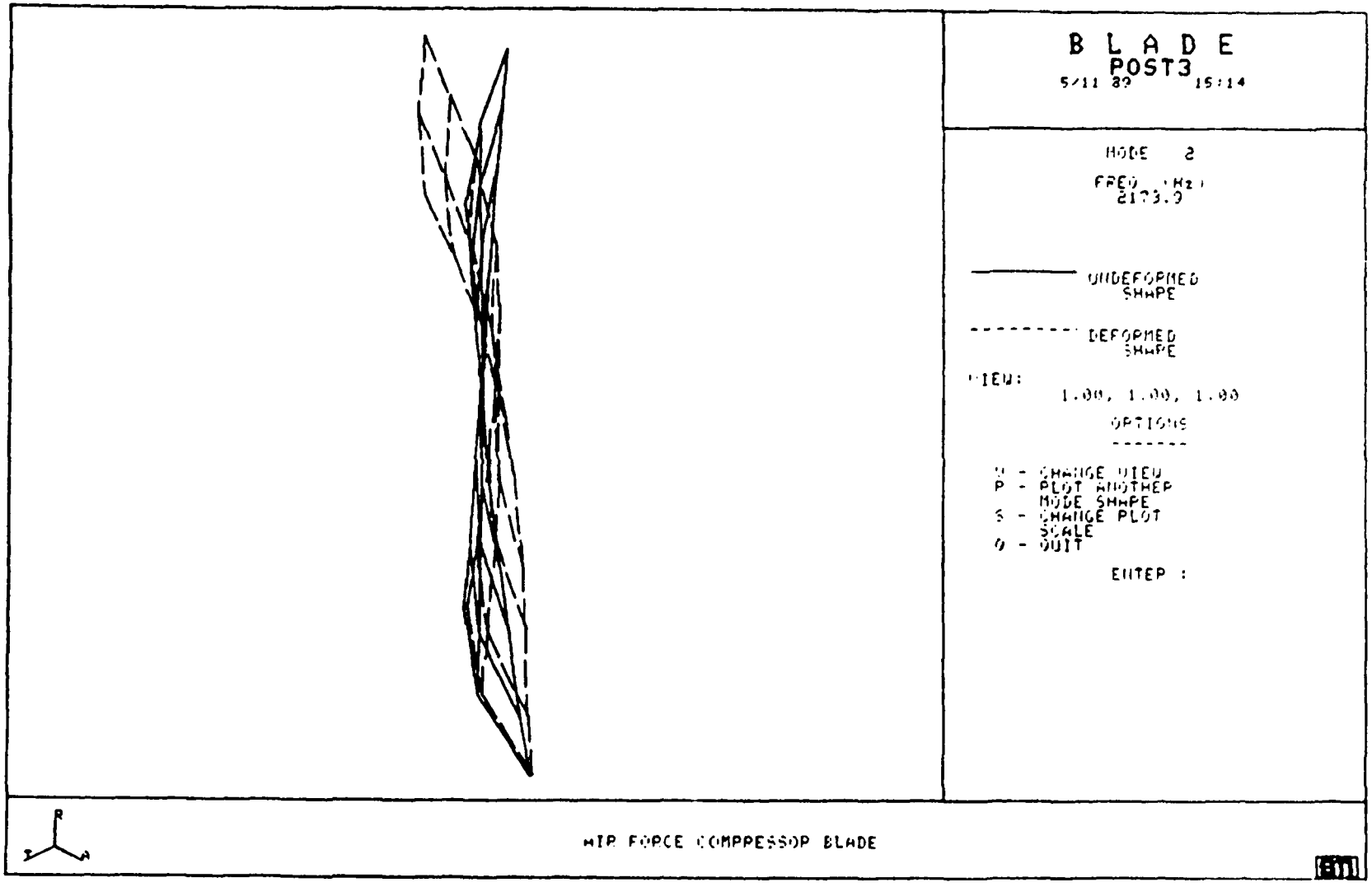

Figure 3.2.2: Mode Shape 2

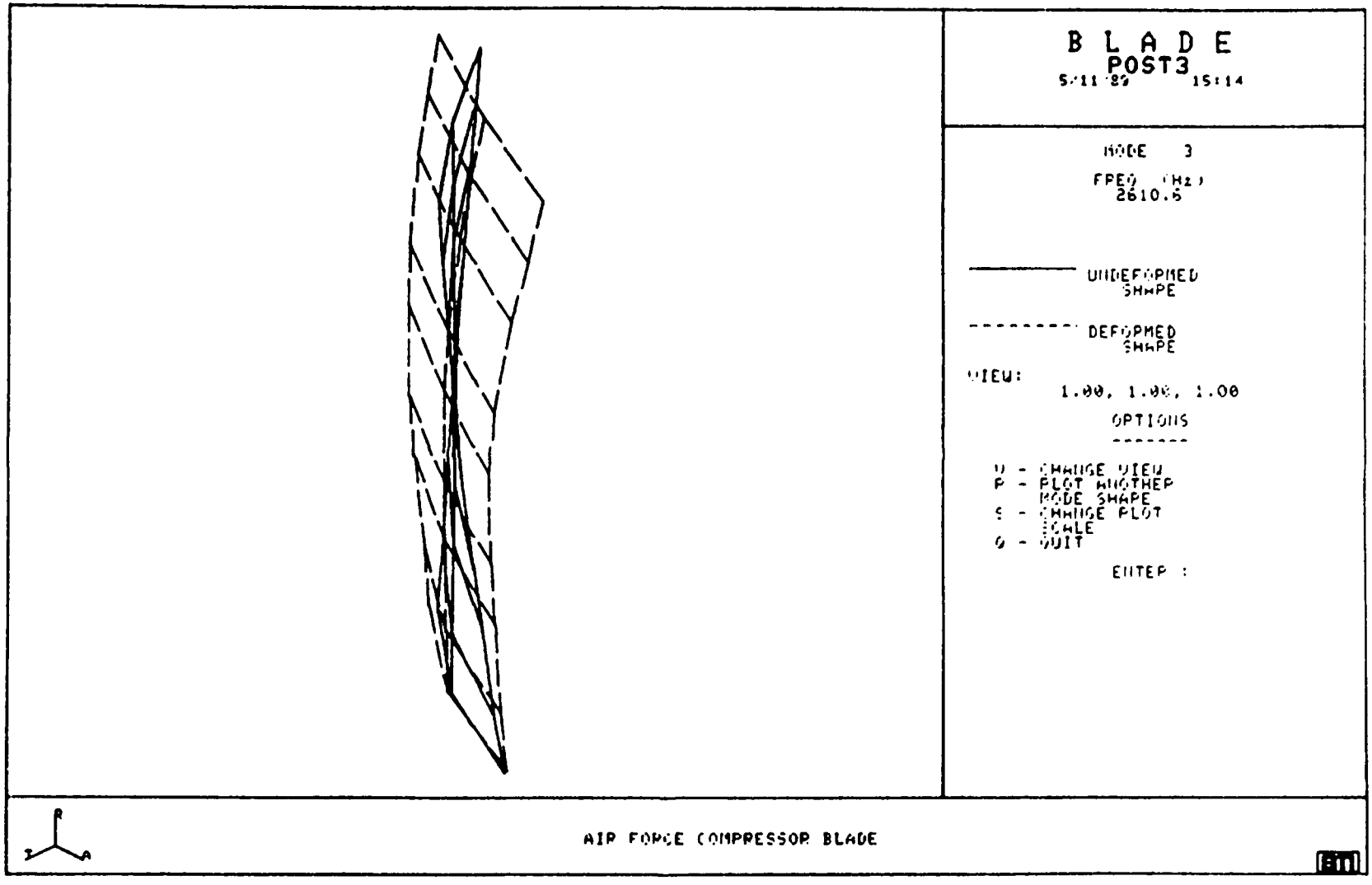

Figure 3.2.3: Mode Shape 3

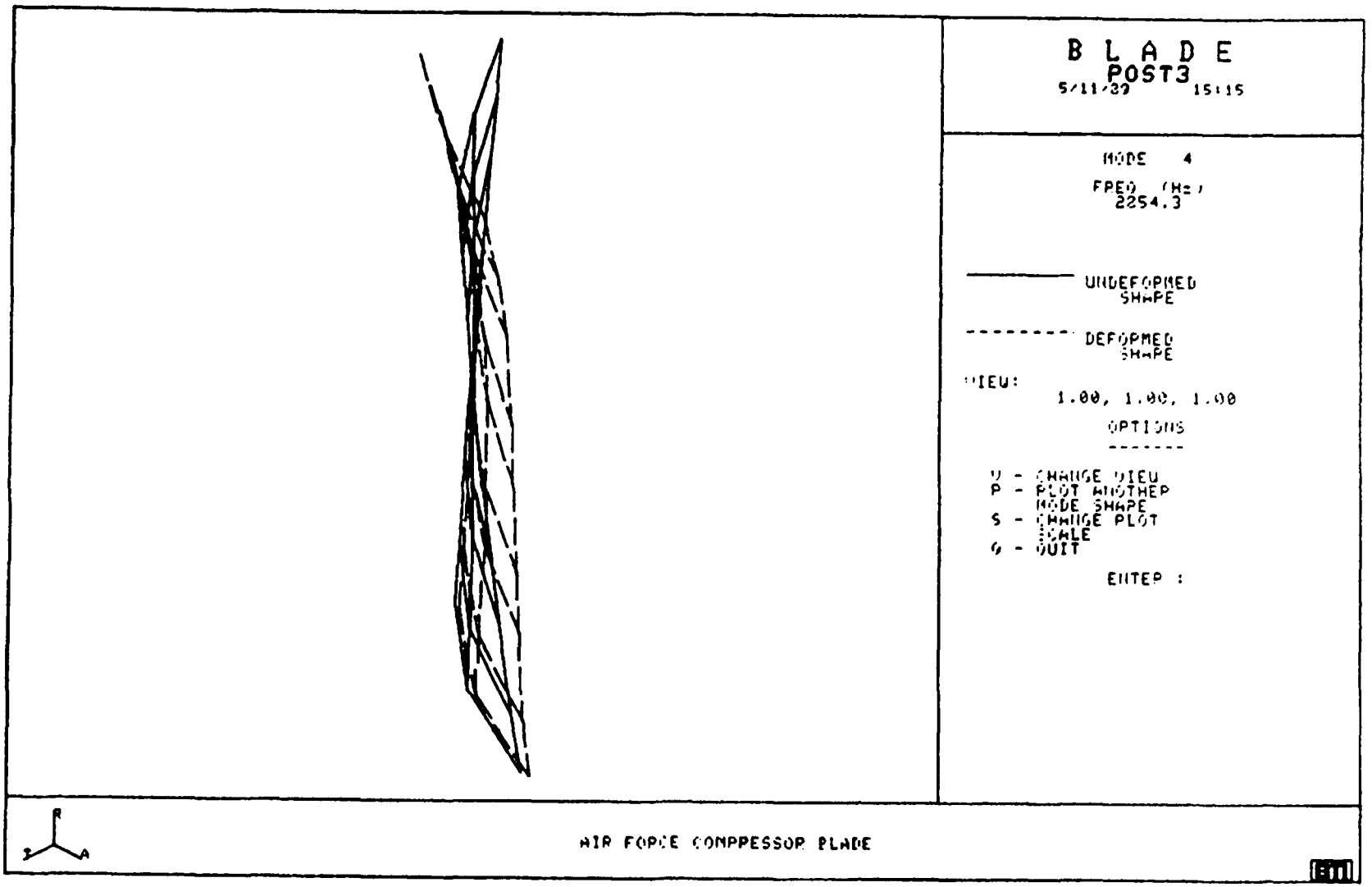

Figure 3.2.5: Mode Shape 4

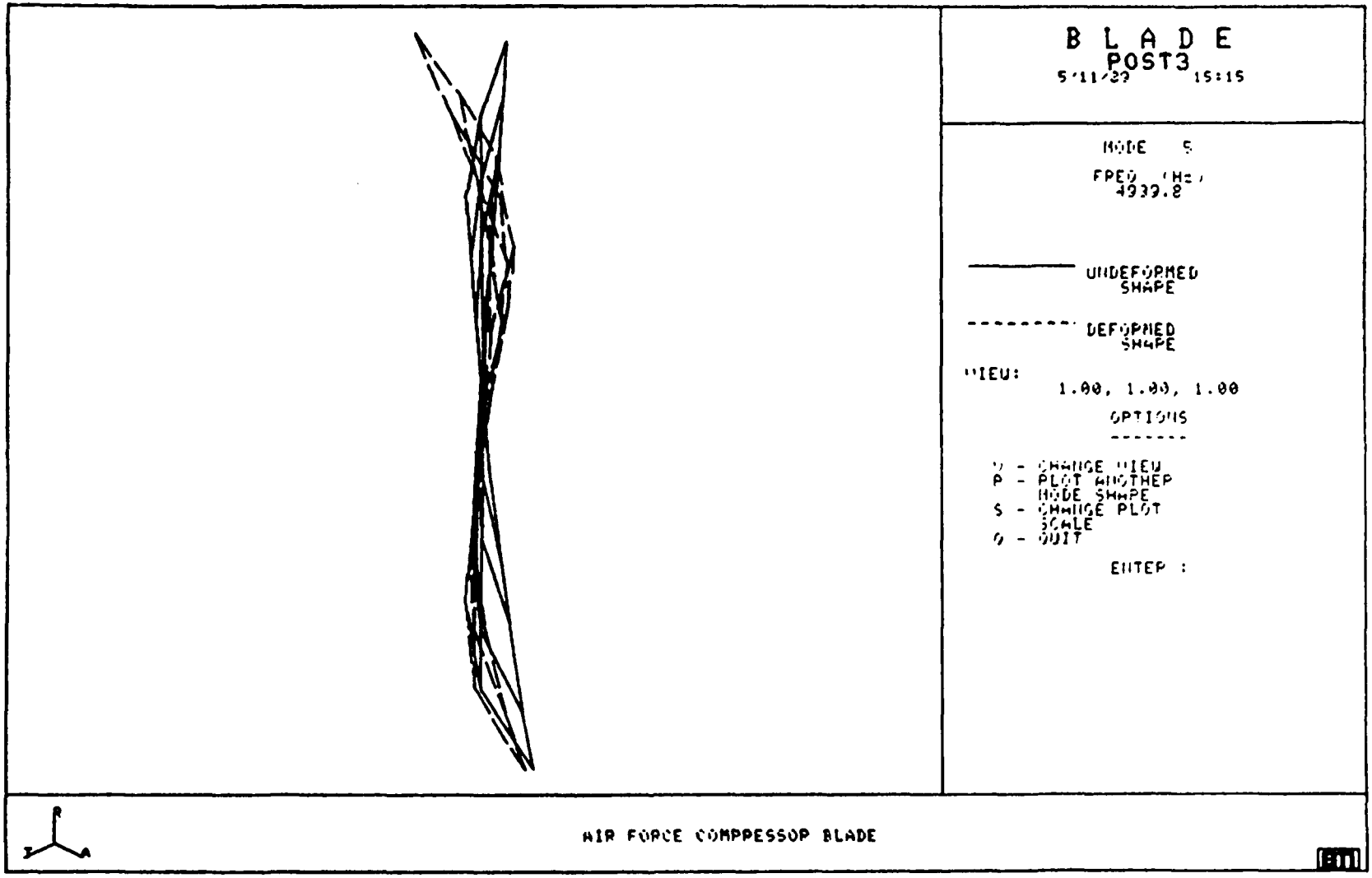

Figure 3.2.5: Mode Shape 5

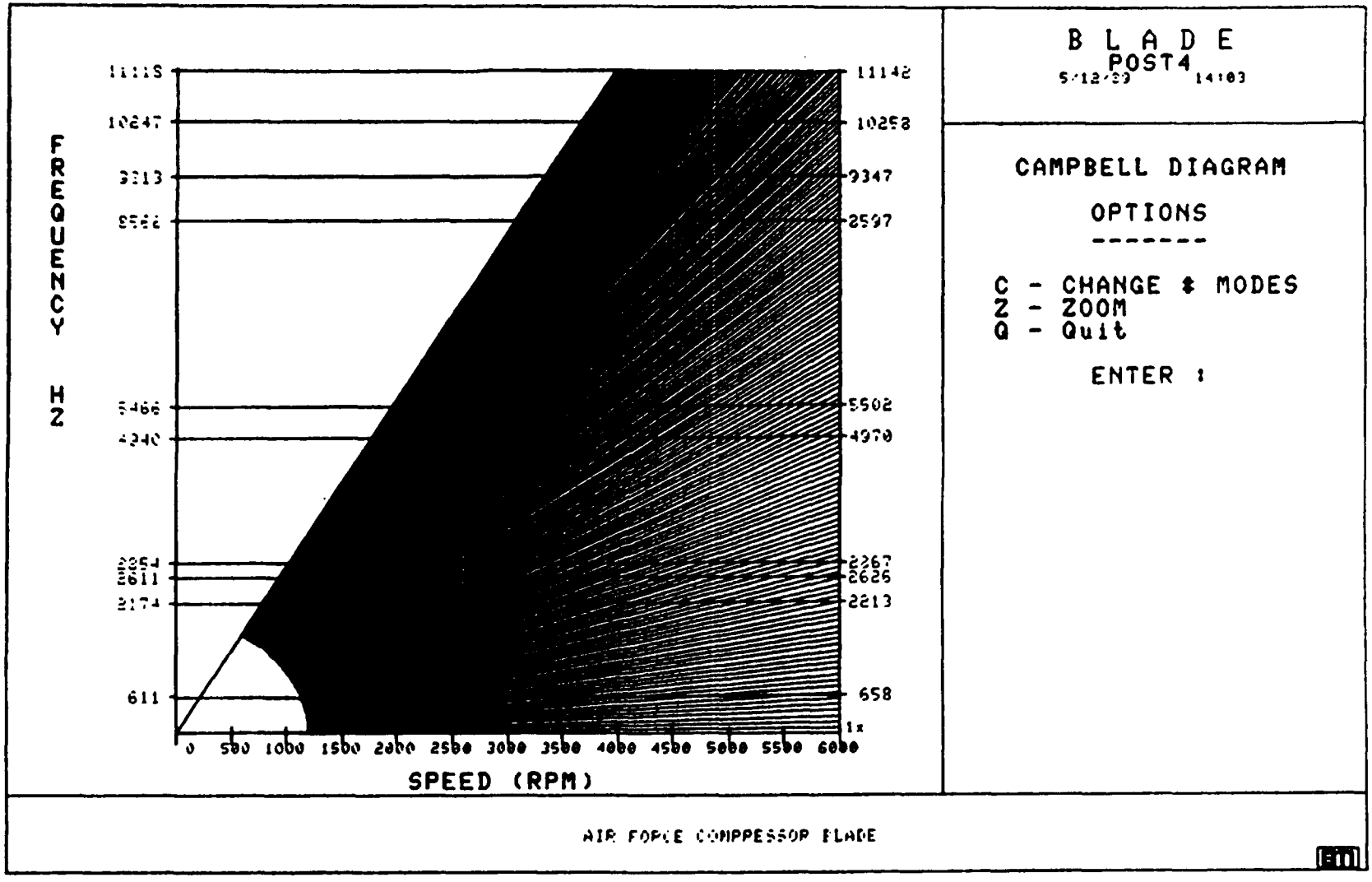

Figure 3.2.6: Campbell Diagram

3.3 Comparison with Test Results

Test results for natural frequencies test data were provided by AFWAL in the form of Holographic photos. The BLADE program was utilized to plot the displacement contours for the different mode shapes. Comparison of the calculated natural frequencies to the test data is given in Table 3.3.1. For Titanium material, it is known that the elastic modulus is strongly dependent on the thermal-mechanical processing. For bar stock, elastic modulus is about $16X10^6$ psi. For forged blade vane, the modulus of elasticity could become $18.0X10^6$ psi. As a result, the blade natural frequency can vary as much as 5 percent. As a matter of fact, the modulus for Titanium changes for one blade from one component to the next as shown in Table 3.3.2 obtained from tests conducted by Westinghouse. The analysis was carried out using a modulus of $17.0X10^6$ psi as shown in Table 3.3.1 in column (2). They compare favorably with the test data as shown by the percentage deviation in column (3). The table also shows that mode 4, 7, and 9 were missing from the experimental data. The Holograms are next compared to the calculated displacement contours in Figures 3.3.1 through Figures 3.3.8.

Table 3.3.1: Comparison of Calculated Frequencies and Test Data

Test Frequency hz	Calculated Frequency hz	% Deviation
602	611.0	+1.5
2138	2173.8	+1.67
2701	2610.6	-3.35
missed	2854.3	----
5200	4939.8	-5.0
5536	5466.2	-1.26
missed	8565.8	----
9480	9313.4	-1.76
missed	10247.0	----
10800	11118.0	+2.90
12620	12865.0	+1.94

Table 3.3.2: Dynamic Modulus of Prototype TI-6AL-4V Blades

Row Number	Location	Direction	Average Dynamic Tensile Modulus (ksi)
1	Airfoil	long	17.61
1	Root	long	17.33
1	Root	trans.	18.10
2	Airfoil	long	17.38
2	Airfoil	trans.	17.71
2	Root	trans.	17.97

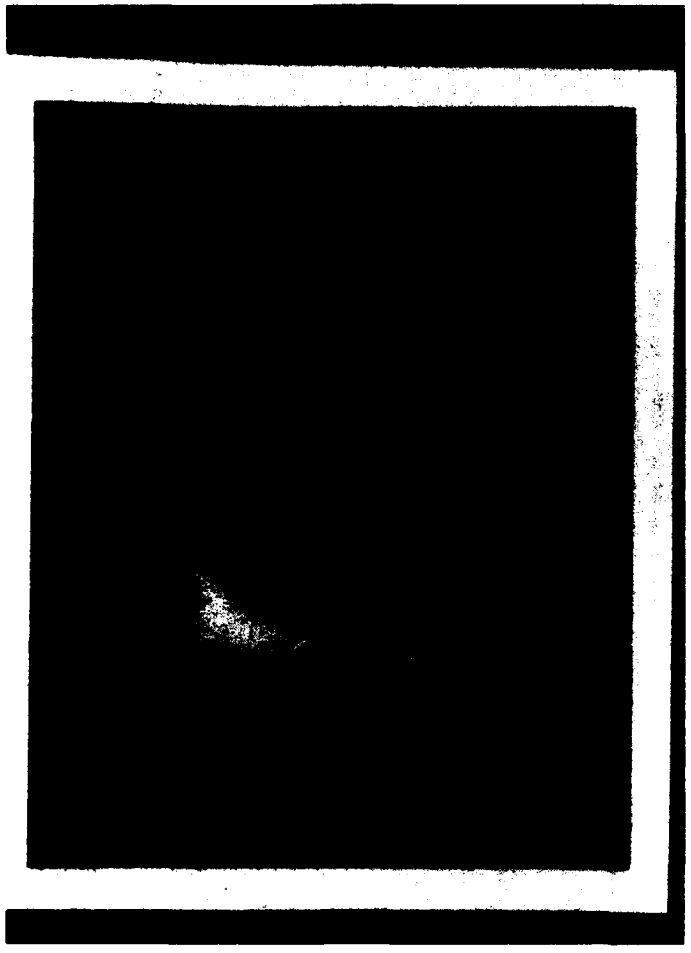

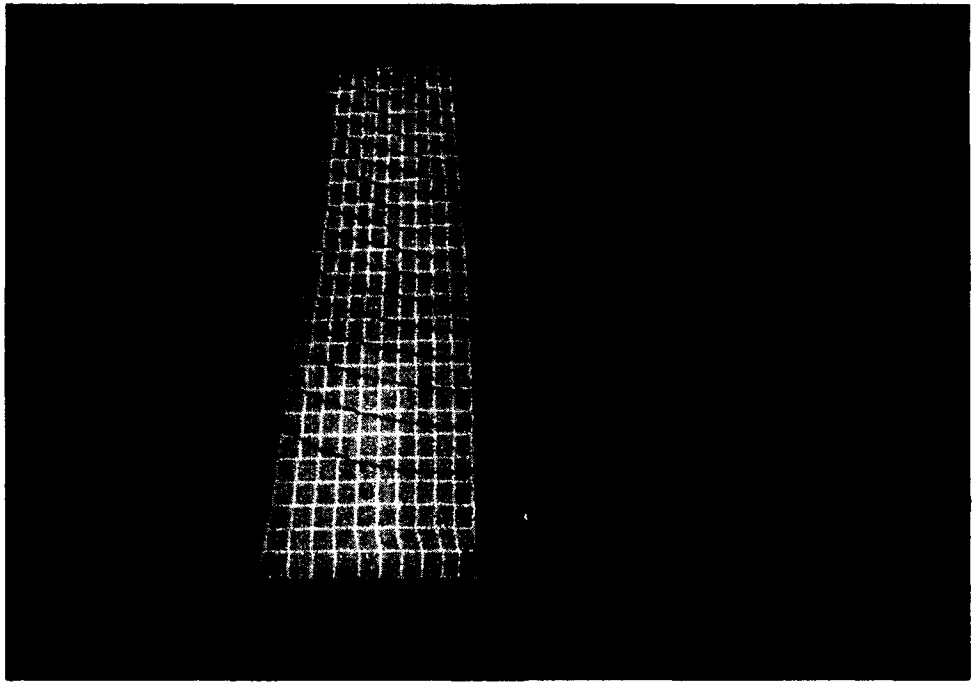

Figure 3.3.1: Comparison of Test Holograms and Analytical Results for Mode 1

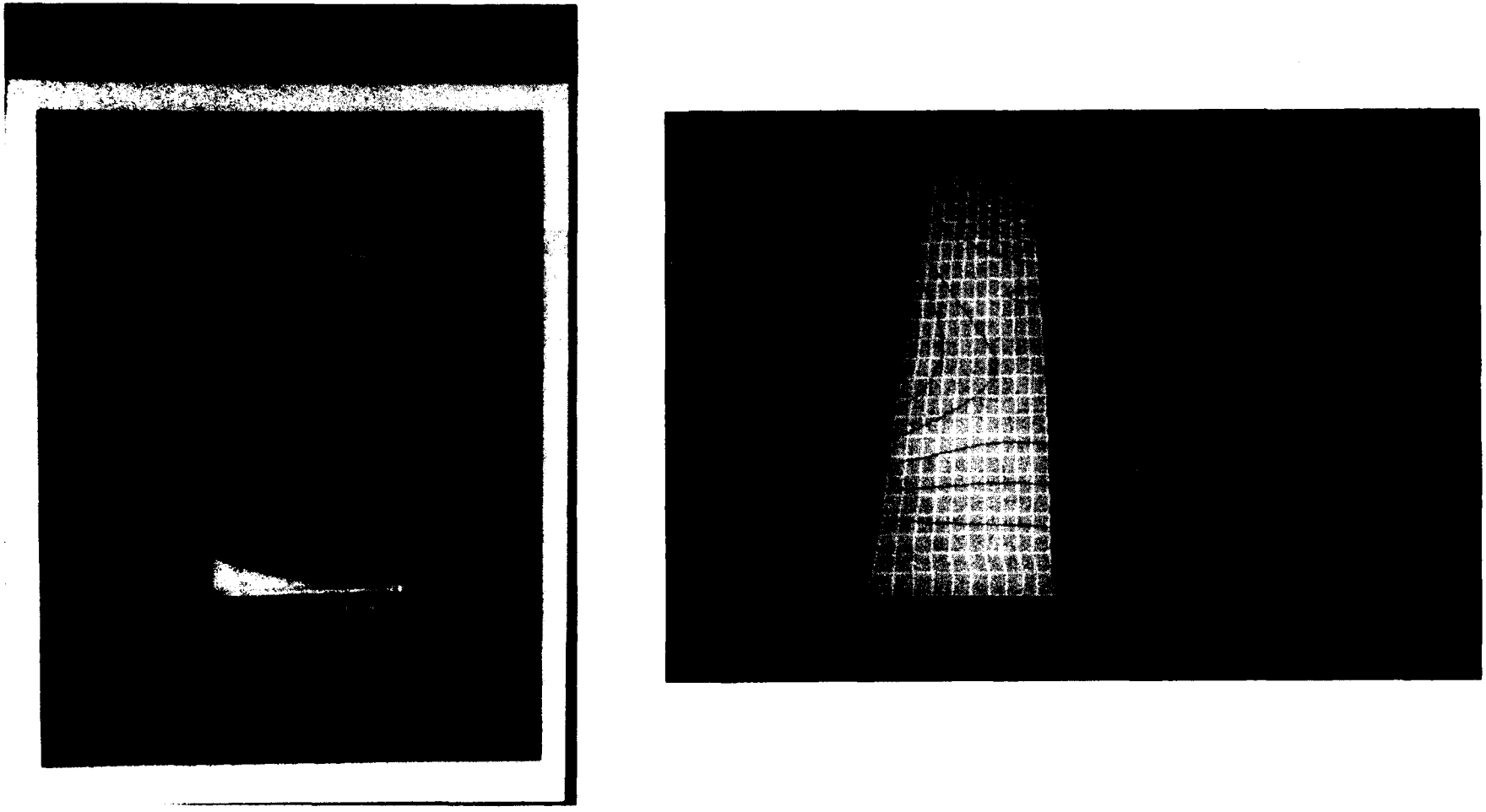

Figure 3.3.2: Comparison of Test Holograms and Analytical Results for Mode 2

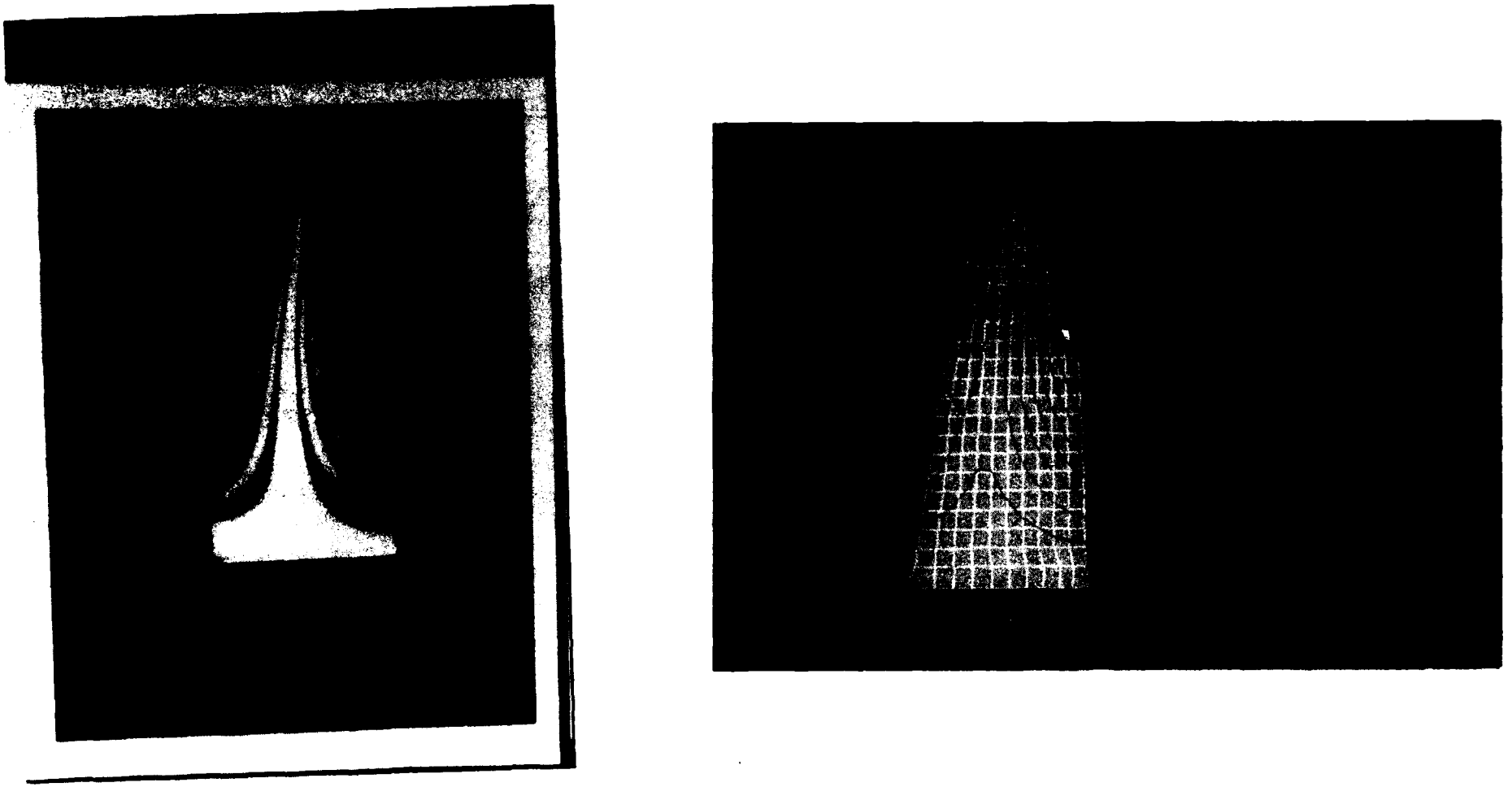

Figure 3.3.3.: Comparison of Test Holograms and Analytical Results for Mode 3

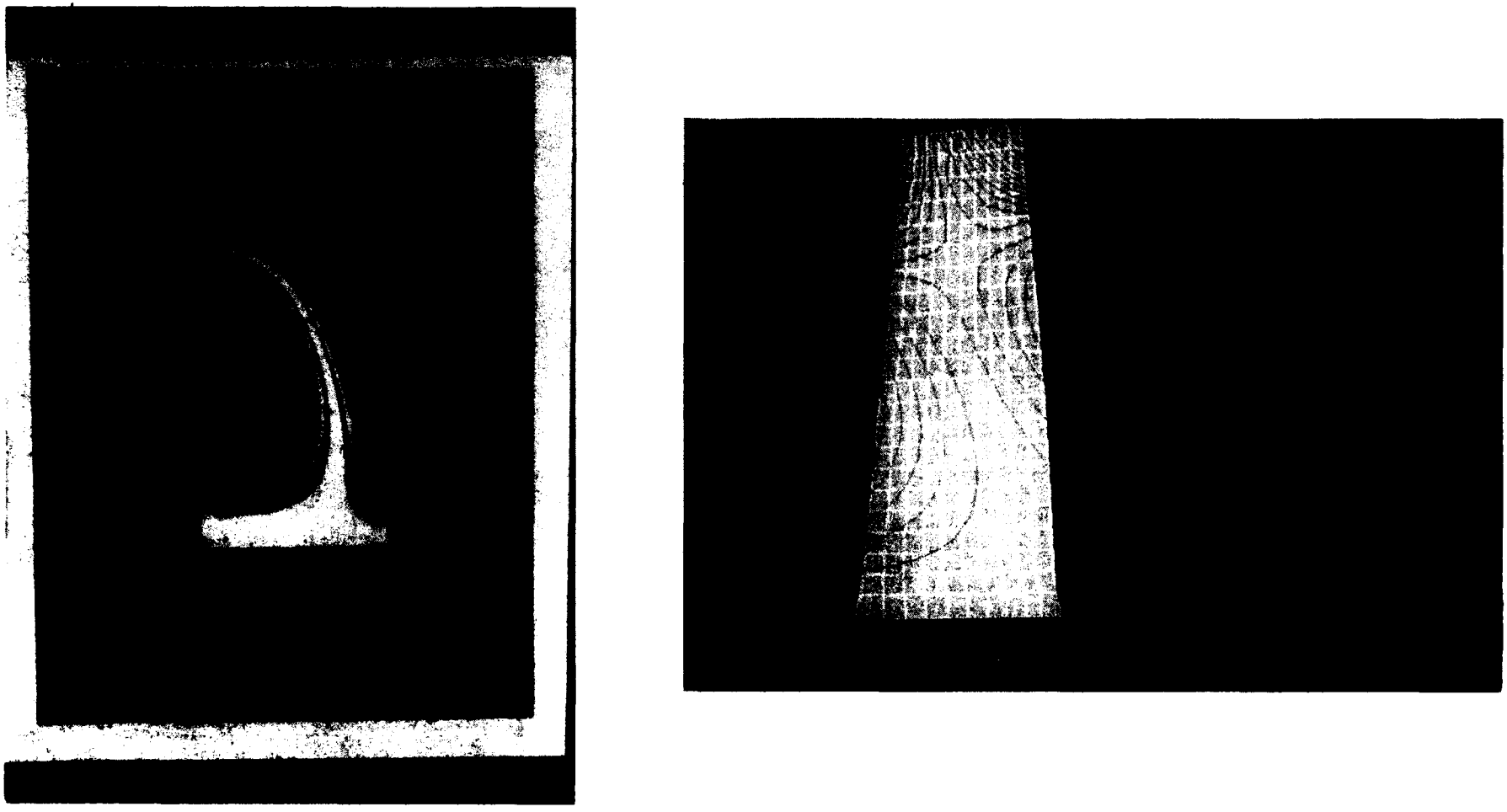

Figure 3.3.4: Comparison of Test Holograms and Analytical Results for Mode 5

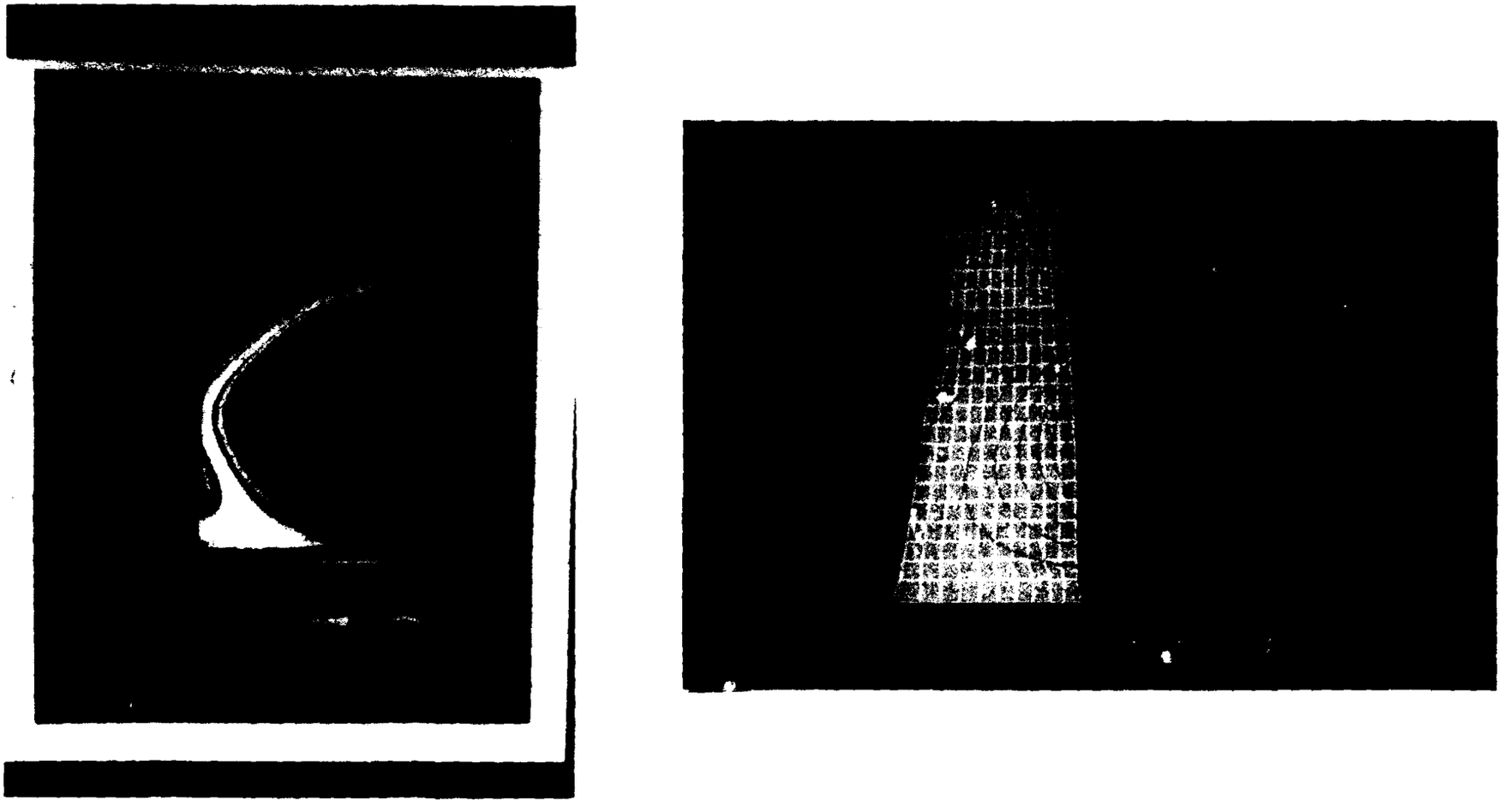

Figure 3.3.5: Comparison of Test Holograms and Analytical Results for Mode 6

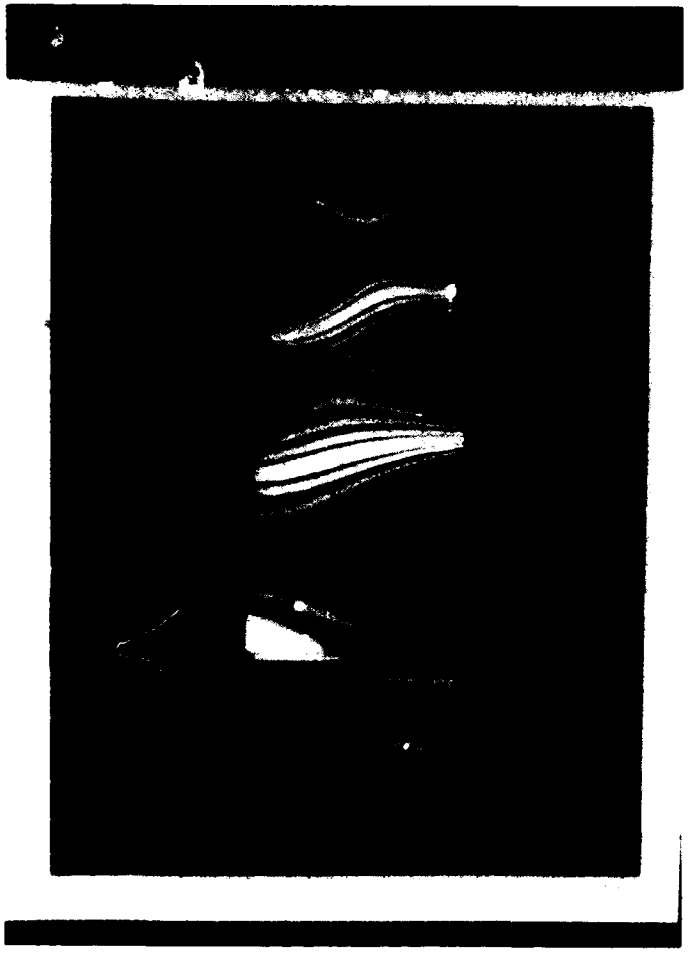

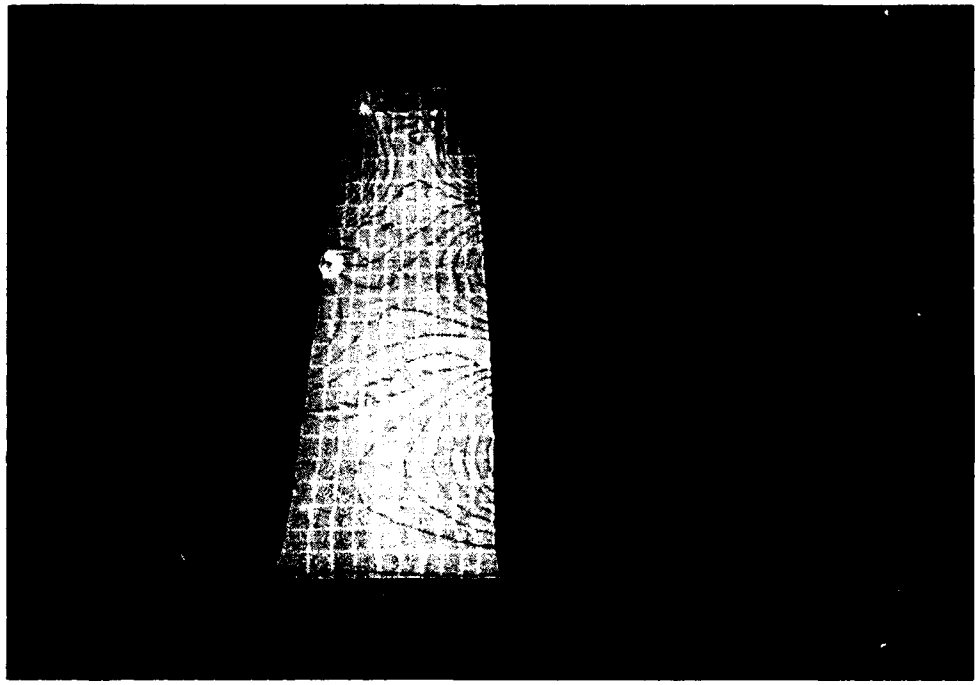

Figure 3.3.6: Comparison of Test Holograms and Analytical Results for Mode 8

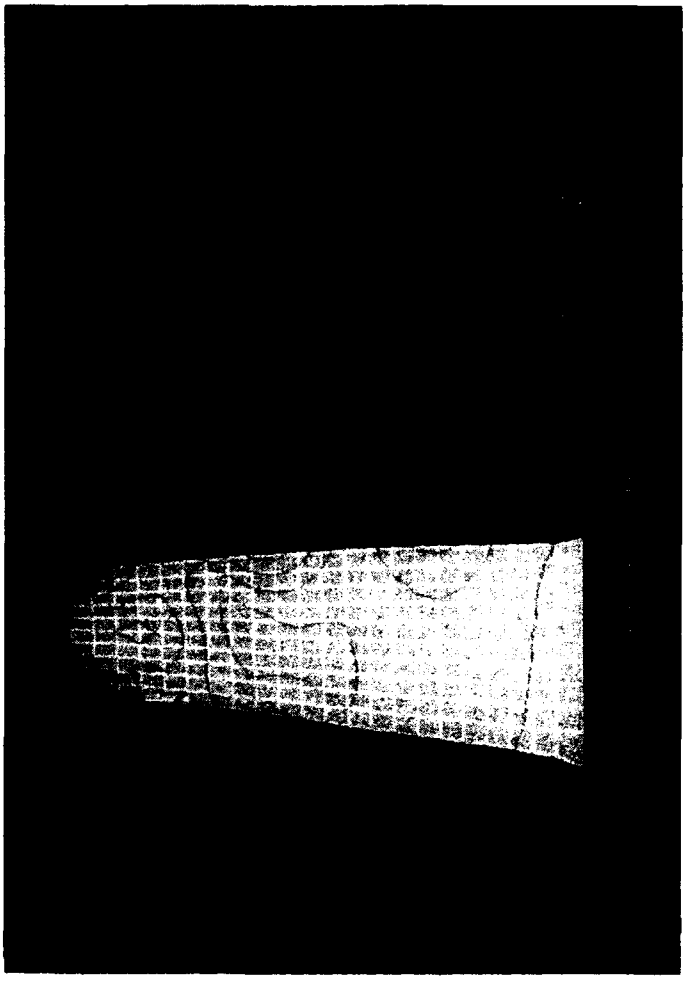

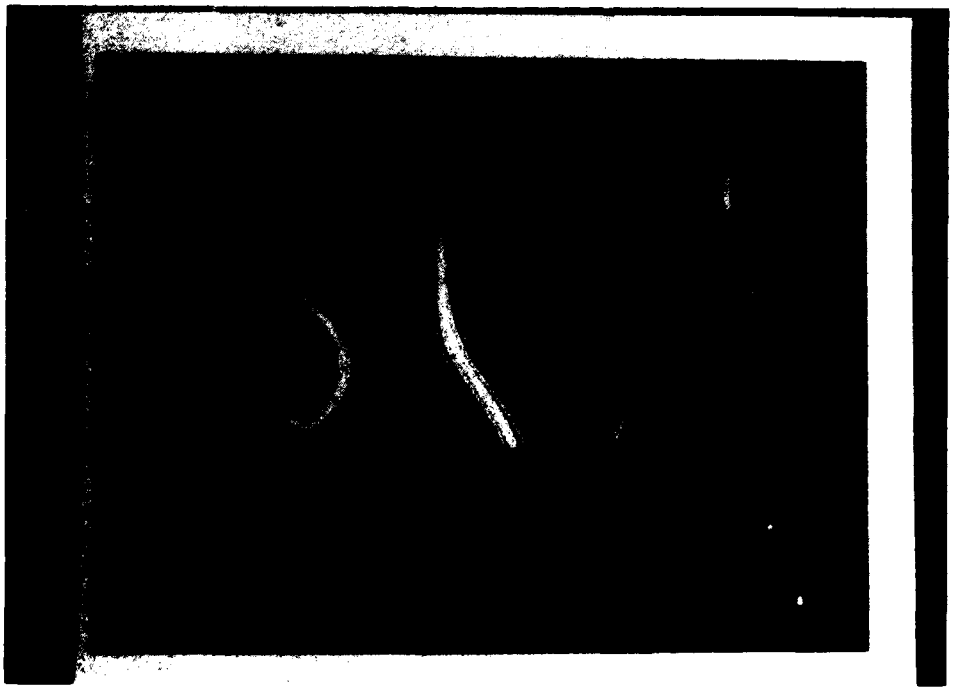

Figure 3.3.7: Comparison of Test Holograms and Analytical Results for Mode 10